Supporting Information

4-Hydroxybenzaldehyde derived Schiff base gelators: Case of sustainability or rupturing of imine bonds towards selective sensing of Ag^+ and Hg^{2+} ions

Atanu Panja and Kumaresh Ghosh*

Department of Chemistry, University of Kalyani, Kalyani, Nadia-741235, India,
Email: ghosh_k2003@yahoo.co.in, kumareshchem18@klyuniv.ac.in, Fax: +91 33258282

Table S1: List of different Hg^{2+} ion responsive supramolecular gelators

Structure	Solvent	Phase transformation in presence of Hg^{2+} ions	Interfering metal ions	Detection limit for Hg^{2+} (M)	Ref.
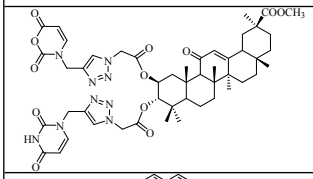	1,2-dichloroethane	Gel to Sol	-	-	*Org. Lett.,* 2011, **13**, 3372.
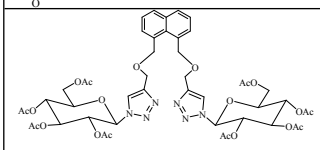	1,2-dichloroethane	Gel to Sol	-	-	*New J. Chem*., 2013, **37**, 2419.
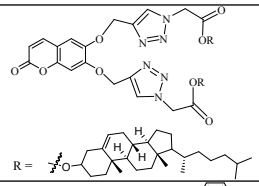	$CHCl_3$:CH_3OH (2:1, v/v)	Gel to Sol	Cu^{2+}, Ag^+	-	*New. J. Chem*., 2016, **40**, 3476.
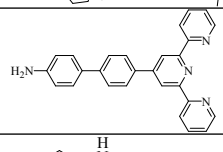	0.2 N HCl	Sol to gel	-	-	*Chem. Commun*., 2014, **50**, 734.
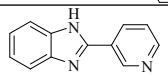	DMSO : H_2O = (1 : 6, v/v)	Gel to Sol	Cu^{2+}, Ag^+	2.02 x 10^{-6}	*Mater. Chem. Front.*, 2018, **2**, 385.
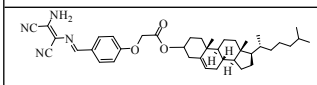	DMF : H_2O = (1 : 1, v/v)	Gel to Sol	Cu^{2+}	2.61 x 10^{-6}	*New. J. Chem*., 2018, DOI:10.1039/C8NJ02426J.
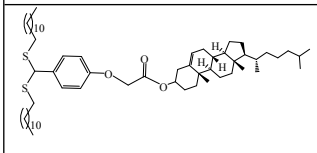	DMF : H_2O = (1 : 1, v/v)	Sol to gel Chemodosimetric approach	-	5.71 x 10^{-6}	*Supramol. Chem.,* 2018, **30**, 722.
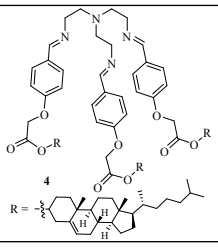	DMF : H_2O = (1 : 1, v/v)	Sol to gel Chemodosimetric approach	-	5.51 x 10^{-6}	*Present work*

Table S2: List of different Ag^+ ion responsive supramolecular gelators

Structure	Solvent	Phase transformation in presence of Ag^+ ions	Interfering metal ions	Detection limit for Ag^+ (M)	Ref.
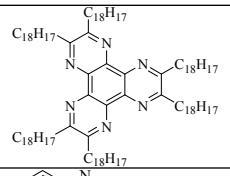	EtOH	Gel to sol	-	-	*Tetrahedron Lett*. 2012, **53**, 1840.
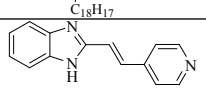	MeOH	Sol to gel	-	-	*Chem. Commun*. 2013, **49**, 4181.
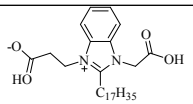	MeOH:H_2O (1:1, v/v)	Sol to gel	-	-	*Supramol. Chem*. 2014, **26**, 39.
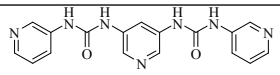	THF/ H_2O	Sol to gel	-	-	*Soft Matter*, 2011, **7**, 2412.
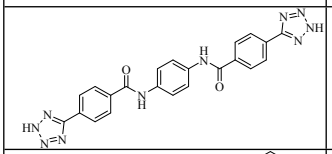	H_2O	Sol to gel	-	-	*Soft Matter*, 2012, **8**, 6557.
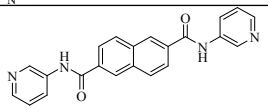	DMF: H_2O (2:3, v/v)	Sol to gel	-	-	*Cryst. Growth Des*. 2015, **15**, 4635.
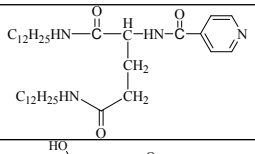	CH_2Cl_2, $CHCl_3$, THF	Sol to gel	-	-	*Langmuir*, 2012, **28**, 27.
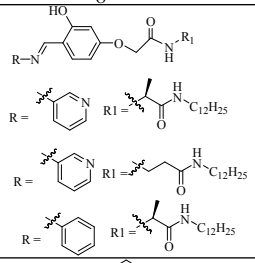	Toluene: EtOH (99:1, v/v)	Sol to gel	-	-	*Chem. Commun*. 2015, **51**, 13929.
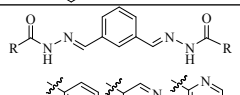	DMF, DMF/ H_2O, DMSO/ H_2O	Sol to gel	-	-	*Cryst. Growth Des*. 2015, **15**, 5360.

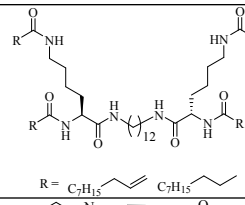	EtOAc	Gel to sol	Li^+	-	*Chem. Commun.* 2012, **48**, 2767.
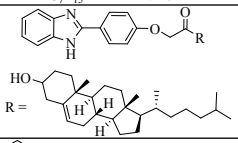	DMF : H_2O (1:1, v/v)	Sol to gel	-	4.31 x 10^{-5}	*ChemistrySelect*, 2017, **2**, 959.
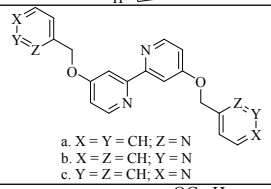	DMSO: H_2O	Sol to gel	-	-	*Dalton Trans*., 2017, **46**, 2793.
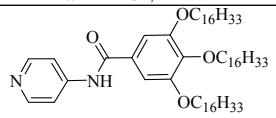	Toluene/ethanol (10:1, v/v)	Sol to gel	-	-	*Langmuir,* 2007, **23**, 8217.
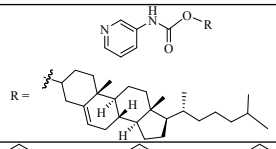	Diphenyl ether	Sol to gel	-	-	*Chem. Lett.*, 2003, **32**, 12.
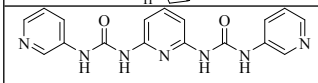	THF-H_2O (3 : 2)	Sol to gel	-	-	*New J. Chem*., 2010, **34**, 2261.
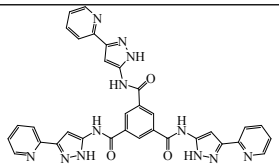	H_2O	Sol to gel	-	-	*New J. Chem*., 2014, **38**, 2470.
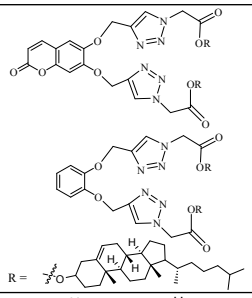	$CHCl_3$:CH_3OH (2:1, v/v)	Gel to Sol	Cu^{2+}, Hg^{2+}	-	*New. J. Chem*., 2016, **40**, 3476.
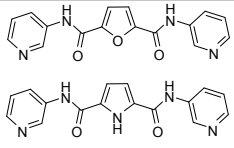	DMSO: H_2O (1:1, v/v)	Sol to gel	Cu^{2+} -	- -	*New. J. Chem*., 2018, **42**, 6488.

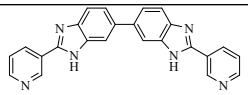	DMSO: H_2O	Gel to sol	Cu^{2+}	3.69 x 10^{-6}	
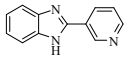	DMSO: H_2O	Gel to sol	Cu^{2+}, Hg^{2+}	3.34 x 10^{-6}	*Mater. Chem. Front.*, 2018, **2**, 385.
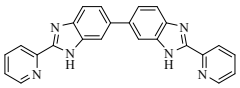	DMSO: H_2O	Sol to gel	-	1.93 x 10^{-7}	
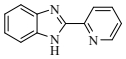	DMSO: H_2O	Sol to gel	-	1.28 x 10^{-6}	
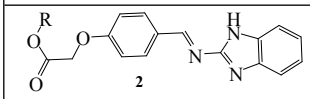 **2**	1,4-dioxane-MeOH (1:1, v/v)	Gel to sol	-	3.27 x 10^{-5}	*Present work*
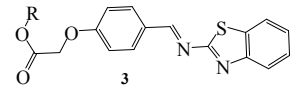 **3**	1,4-dioxane-H_2O (1:1, v/v)	Sol to gel	-	9.27 x 10^{-5}	
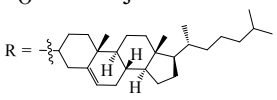					

Table S3: Results of gelation tests for **1-5**

Solvent	**1**	**2**	**3**	**4**	**5**
$CHCl_3$	S	S	S	S	S
2% Methanol in $CHCl_3$	S	S	S	S	S
$CHCl_3$: MeOH (1:1, v/v)	PG	**G** (12 mg/mL)	S	S	S
$CHCl_3$: MeOH (1:2, v/v)	**G** (54 mg/mL)	**G** (9 mg/mL)	P	P	S
THF	S	S	S	S	S
CH_3CN	PS	I	I	PS	**G**
DMSO	PS	I	I	PS	PG
MeOH	I	I	I	I	PS
DMF	S	S	PG	S	S
Petroleum ether	PS	PS	PS	PS	PS
DMF : H_2O (1:1, v/v)	P	P	P	P	**G**
1,4-Dioxane : H_2O (1:1, v/v)	P	S	P	P	PG
DMSO : H_2O (1:1, v/v)	P	P	P	I	P
1,4-Dioxane : MeOH (1:1, v/v)	P	**G** (5 mg/mL)	P	-	PG
1,4-Dioxane : H_2O (1:1, v/v) + Ag^+	P	P	**G** (8 mg/mL)	P	P
1,4-Dioxane : H_2O (1:1, v/v) + Cu^{2+}	P	P	P	P	P
DMF + Ag^+	S	S	PG	S	-
DMF + Cu^{2+}	S	S	PG	S	-
DMF : H_2O (1:1, v/v) + Ag^+	P	P	P	P	-
DMF : H_2O (1:1, v/v) + Cu^{2+}	P	P	P	P	-
S = solution; G = gel (mgc); I = insoluble; PS = partially soluble; P = Precipitation, PG = partial gel (thick material did not stick on the top of the vial upon turning). Gels were primarily identified by inversion of vials after 20-30 mins.					

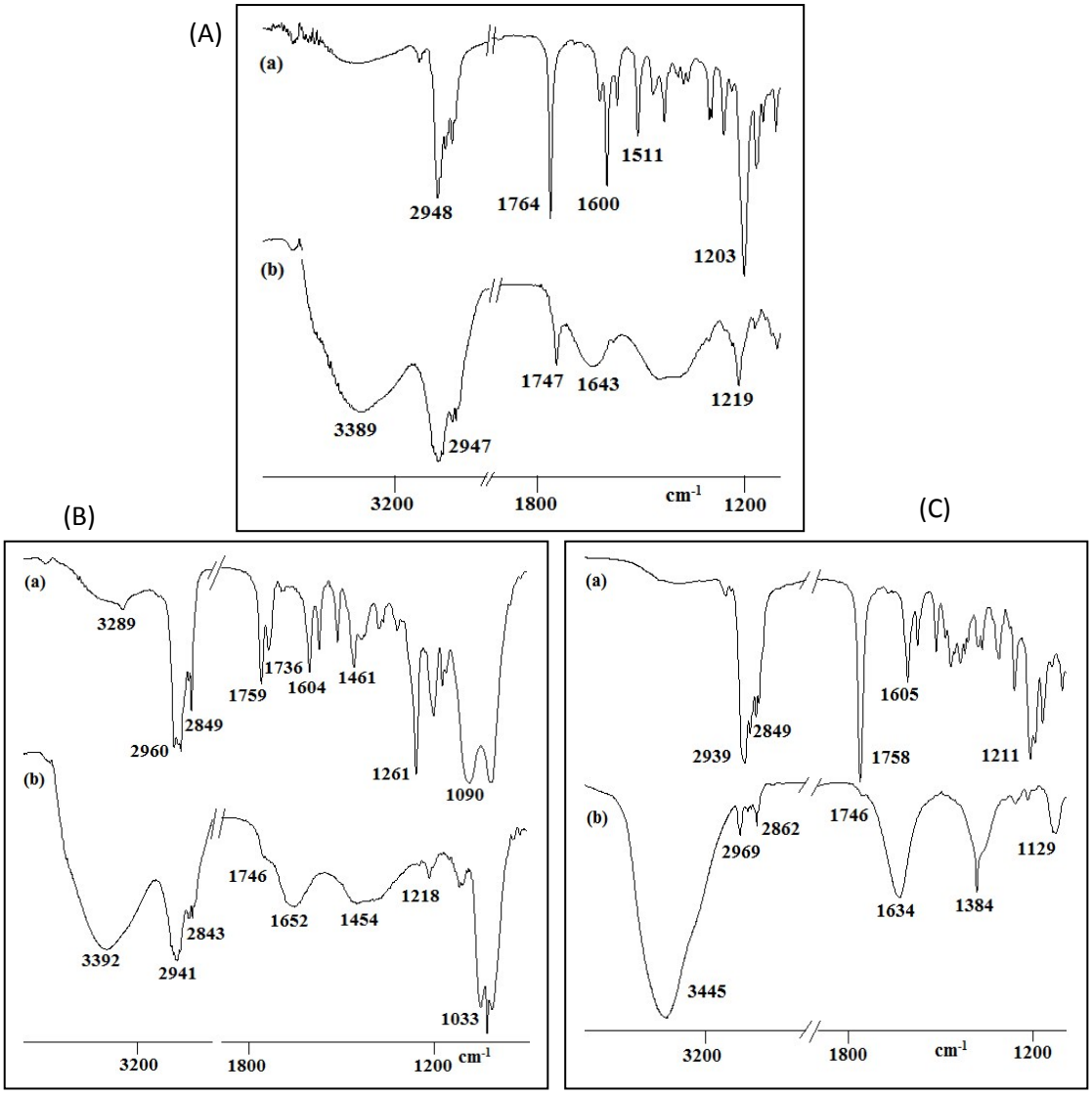

Fig. S1. Partial FTIR spectra of (A) **1**, (B) **2** and (C) **3** in (a) amorphous and (b) gel states [Gels were prepared from $CHCl_3$/MeOH (1:2, v/v) for **1** and 1,4-Dioxane/MeOH (1:1, v/v) for **2**. For **3** it was 1,4-Dioxane/H_2O (1:1, v/v) with equiv. amount of Ag^+ ion].

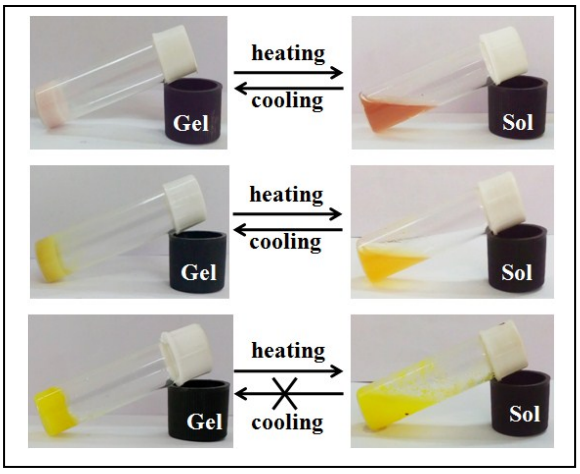

Fig. S2. Photographs showing the thermal responsiveness of the gel of **1** from $CHCl_3$/MeOH (1:2, v/v), **2** from 1,4-Dioxane/MeOH (1:1, v/v) and Ag^+-gel of **3** from 1,4-Dioxane/H_2O (1:1, v/v) (from top to bottom).

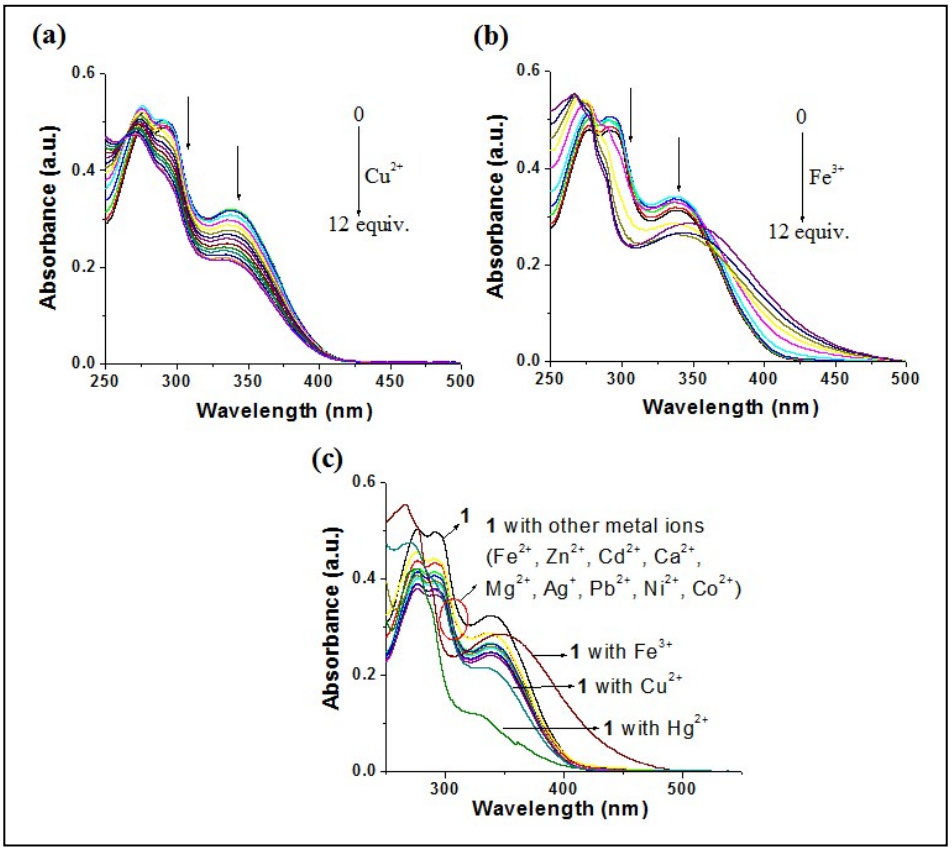

Fig. S3. Change in absorbance of **1** (c = 2.50 x 10^{-5} M) upon addition of 12 equiv. amounts of (a) Cu^{2+}, (b) Fe^{3+} and (c) different metal ions (c = 1.0 x 10^{-3} M) in $CHCl_3$/CH_3OH (1:2, v/v).

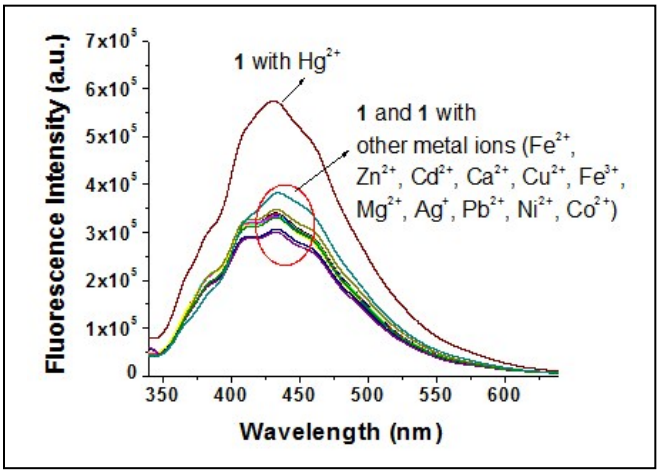

Fig. S4. Change in emission (λ_{ex} = 330 nm) of **1** (c = 2.50 x 10^{-5} M) upon addition of 10 equiv. amounts of different metal ions (c = 1.0 x 10^{-3} M) in $CHCl_3/CH_3OH$ (1:2, v/v).

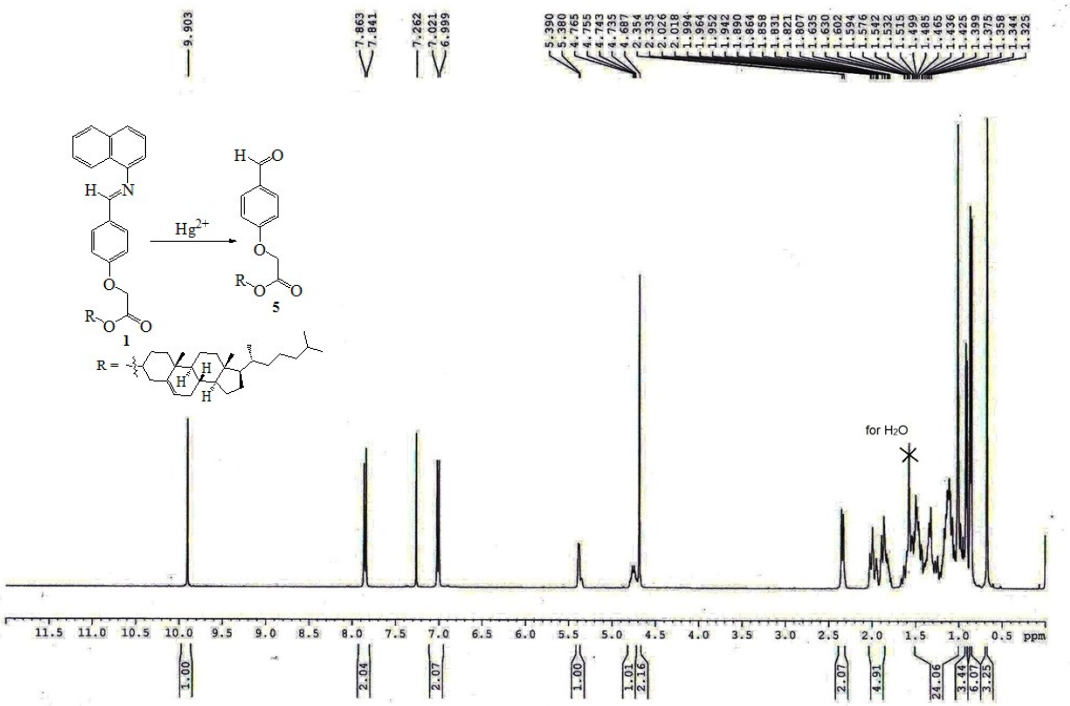

Fig. S5. ^1H NMR spectra ($CDCl_3$, 400 MHz) of the isolated product (compound **5**) obtained from the reaction of **1** with Hg^{2+} ion.

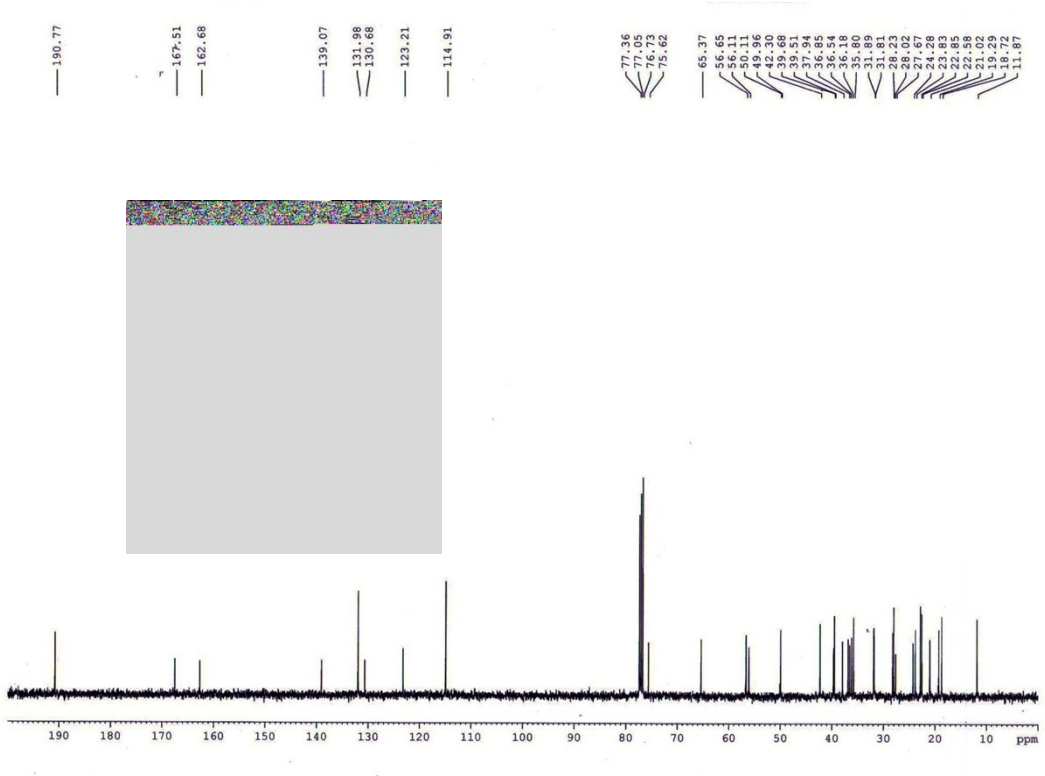

Fig. S6. ^{13}C NMR spectra ($CDCl_3$, 100 MHz) of the isolated product (compound **5**) obtained from the reaction of **1** with Hg^{2+} ion.

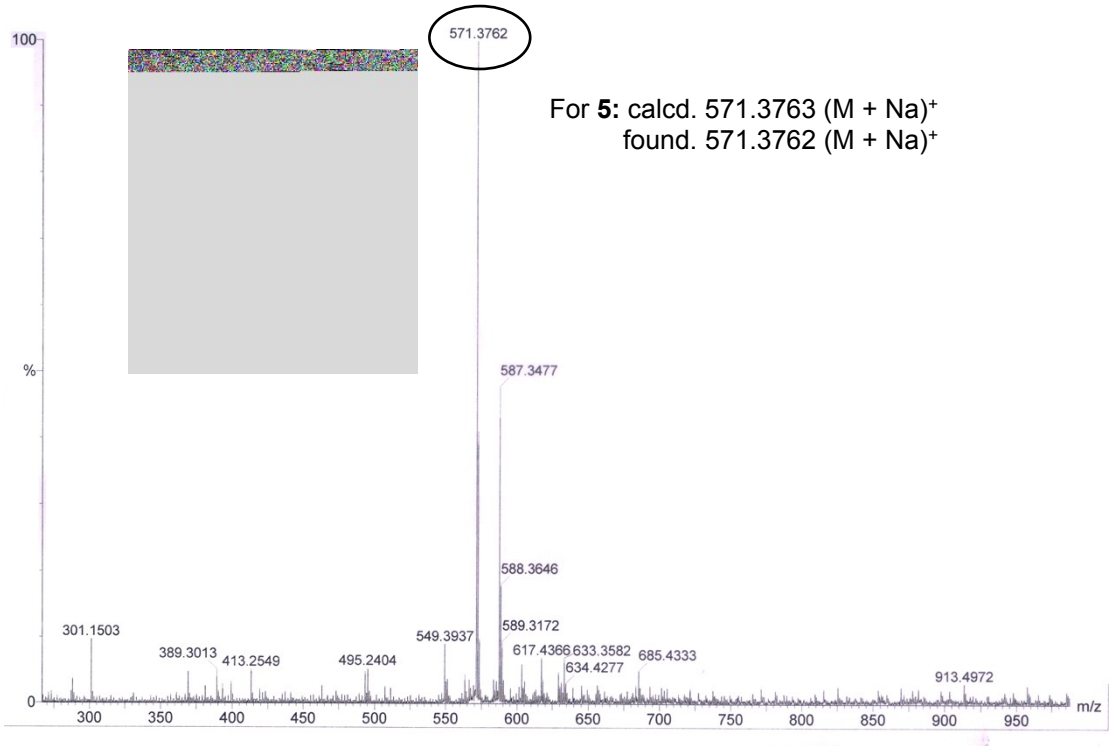

Fig. S7. HRMS spectra of the isolated product (compound **5**) obtained from the reaction of **1** with Hg^{2+} ion.

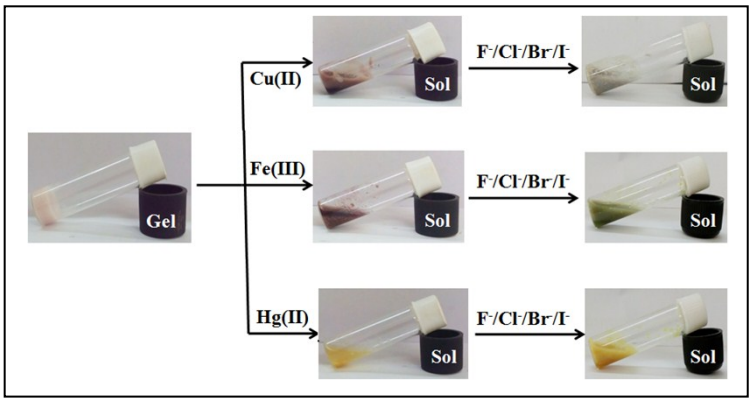

Fig. S8. Chemical responsiveness of the metal ion induced sols of **1** in presence of different halides.

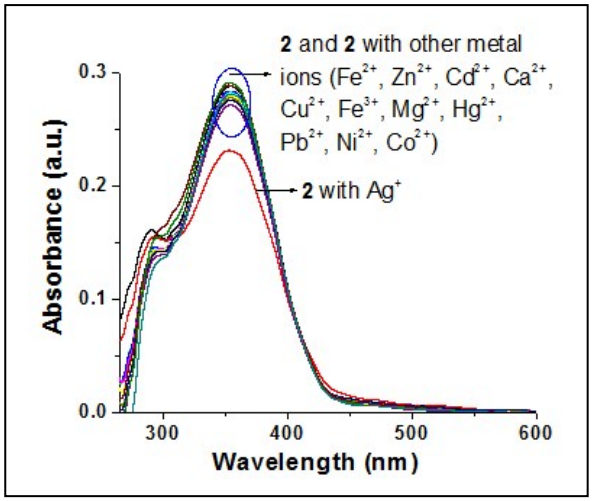

Fig. S9. Change in absorbance of **2** (c = 2.50 x 10^{-5} M) upon addition of 2 equiv. amounts of different metal ions (as perchlorate salt, c = 1.0 x 10^{-3} M) in 1,4-Dioxane/MeOH (1:1, v/v).

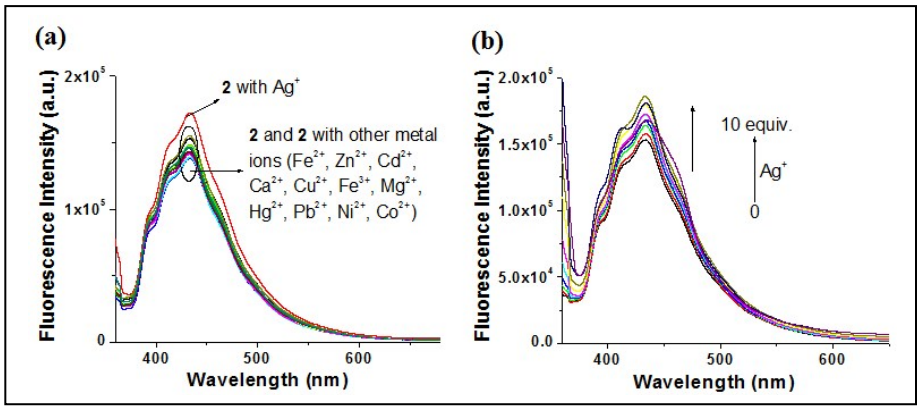

Fig. S10. Change in emission (λ_{ex} = 350 nm) of **2** (c = 2.50 x 10^{-5} M) upon addition of (a) 2 equiv. amounts of different metal ions and (b) 10 equiv. amounts of Ag^+ ions (c = 1.0 x 10^{-3} M) in 1,4-Dioxane/MeOH (1:1, v/v).

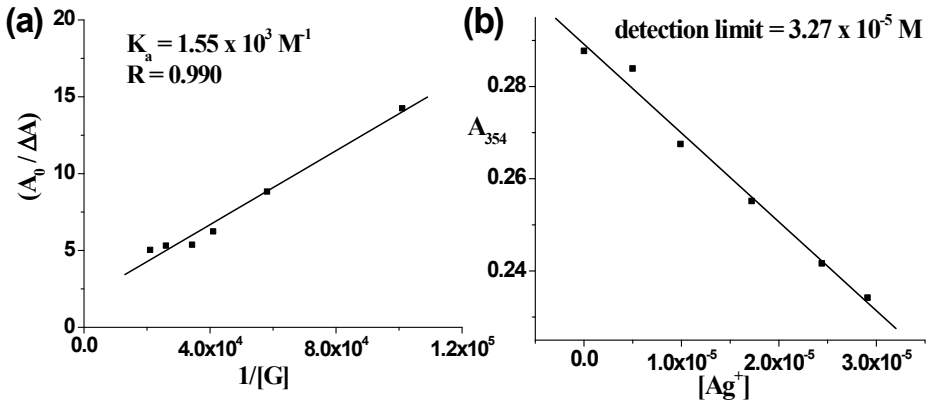

Fig. S11. (a) Benesi–Hilderband plot and (b) detection limit for **2** (c = 2.5 x 10^{-5} M) with Ag^+ ion (c = 1.0 x 10^{-3} M) at 354 nm in 1,4-Dioxane/MeOH (1:1, v/v) from UV-vis titration.

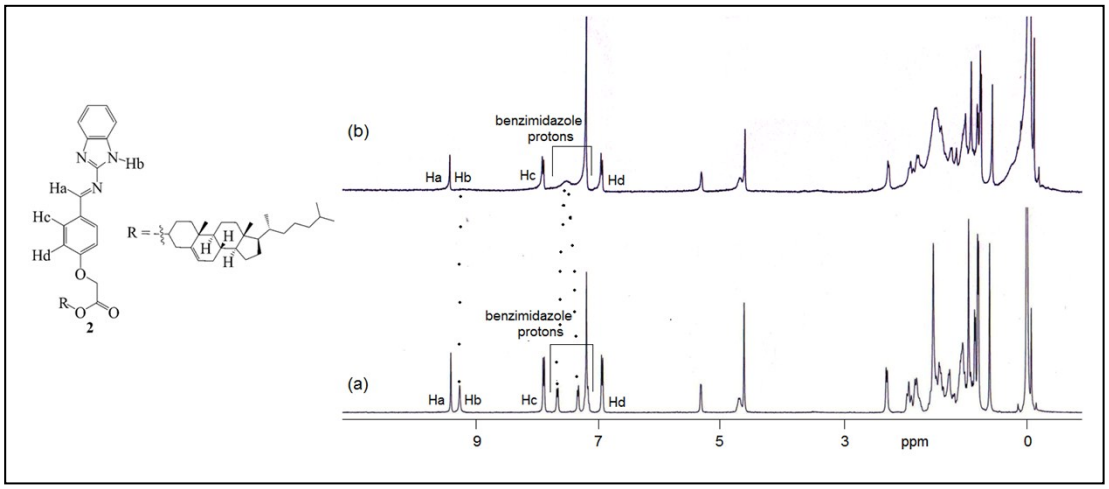

Fig. S12. ^1H NMR spectra of (a) **2** and (b) **2** with Ag^+ ion (1:1, after ~15 mins) in $CDCl_3$.

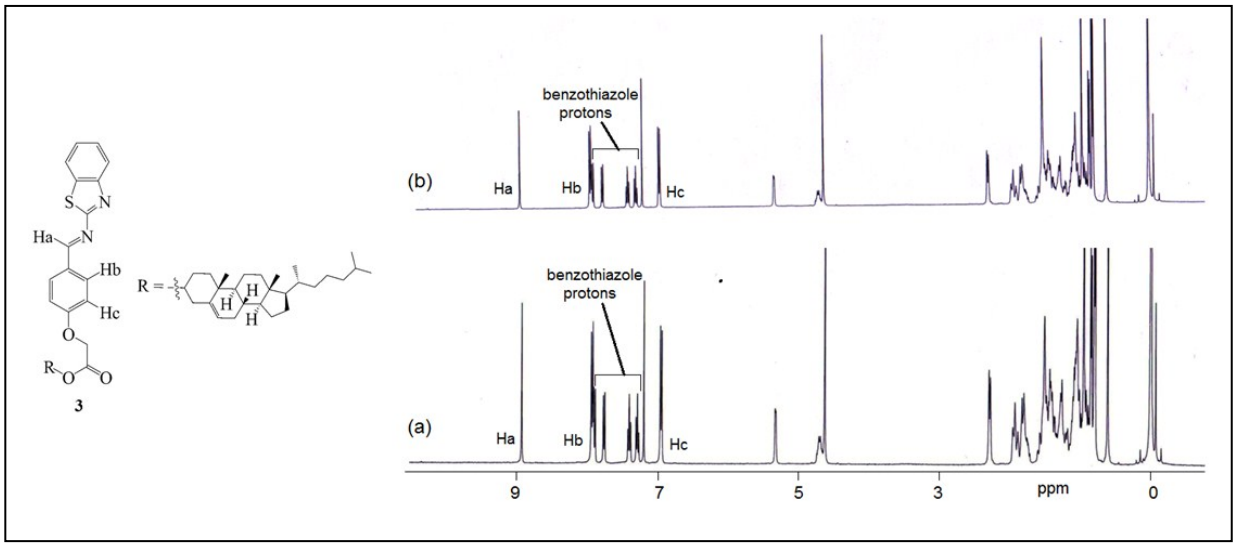

Fig. S13. Partial ^{1}H NMR spectra of (a) **3** and (b) **3** with Ag^{+} ion (1:1, after ~15 mins) in $CDCl_3$.

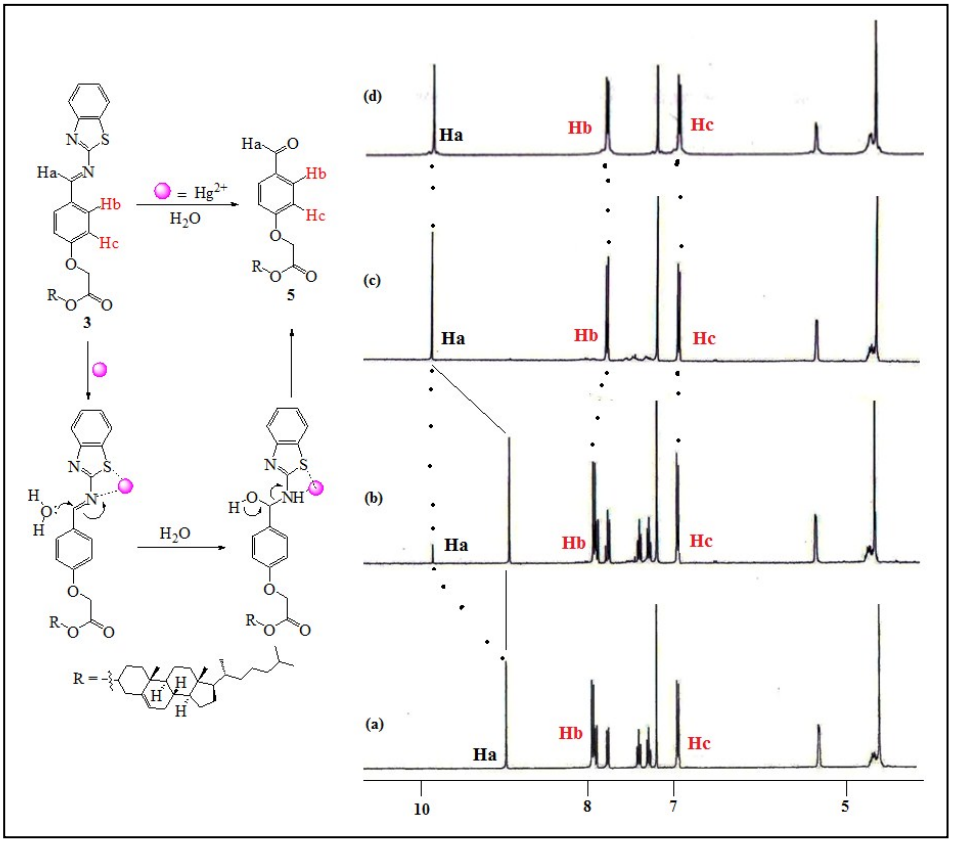

Fig. S14. Partial ^{1}H NMR spectra of (a) **3**, (b) **3** with Hg^{2+} ion (1:1, after ~5 min), (c) **3** with Hg^{2+} ion (1:1, after ~30 min) and (d) **5** itself in $CDCl_3$.

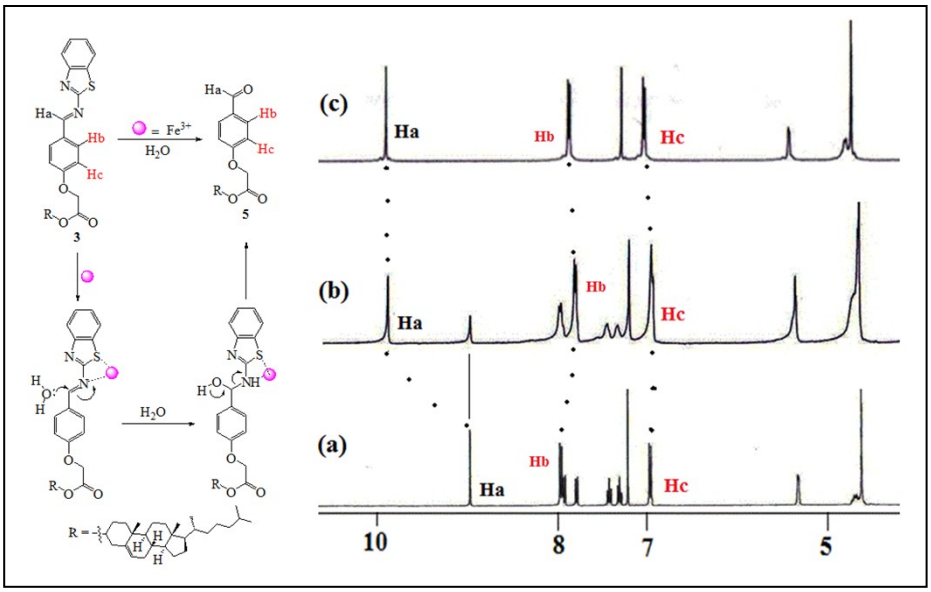

Fig. S15. Partial ^{1}H NMR spectra of (a) **3**, (b) **3** with Fe^{3+} ion (1:1, after ~15 min) and (c) **5** itself in $CDCl_3$.

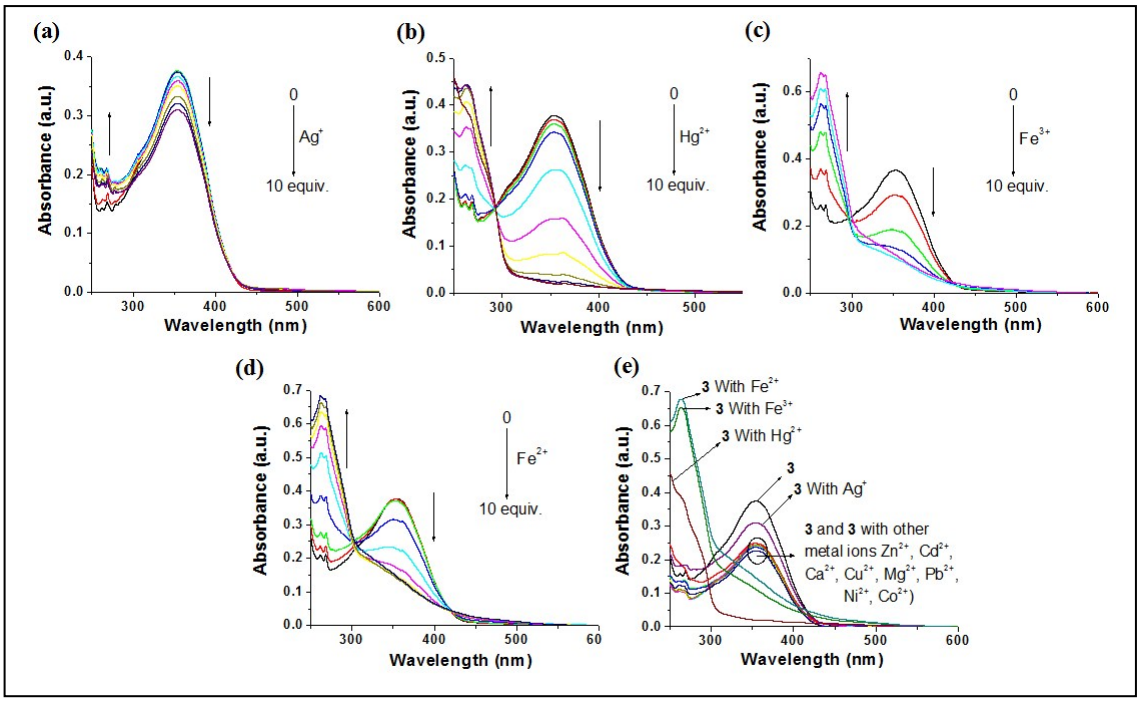

Fig. S16. Change in absorbance of **3** (c = 2.50 x 10^{-5} M) upon addition of 10 equiv. amounts of (a) Ag^+, (b) Hg^{2+}, (c) Fe^{3+}, (d) Fe^{2+} and (e) different metal ions (as perchlorate salts, c = 1.0 x 10^{-3} M) in 1,4-Dioxane/H_2O (2:1, v/v, to avoid precipitation or suspension 2:1 volume ratio was taken).

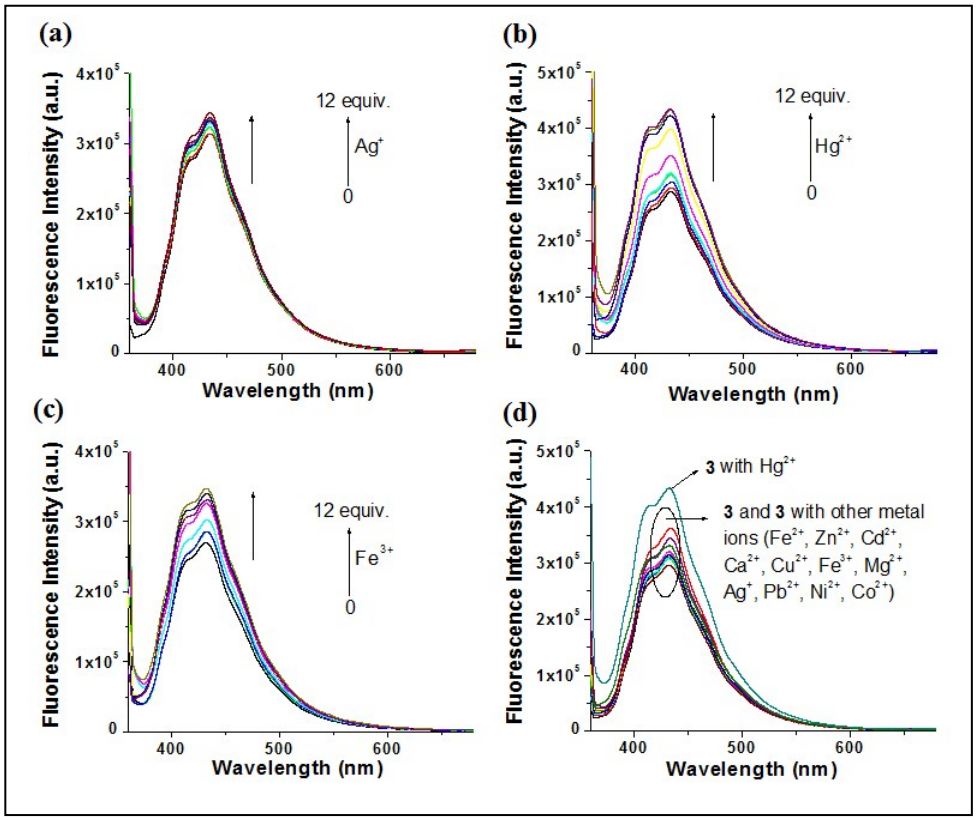

Fig. S17. Change in emission (λ_{ex} = 350 nm) of **3** (c = 2.50 x 10^{-5} M) upon addition of 12 equiv. amounts of (a) Ag^{+}, (b) Hg^{2+}, (c) Fe^{3+} and (d) different metal ions ion (as perchlorate salts, c = 1.0 x 10^{-3} M) in 1,4-Dioxane/H_2O (2:1, v/v, to avoid precipitation or suspension 2:1 volume ratio was taken).

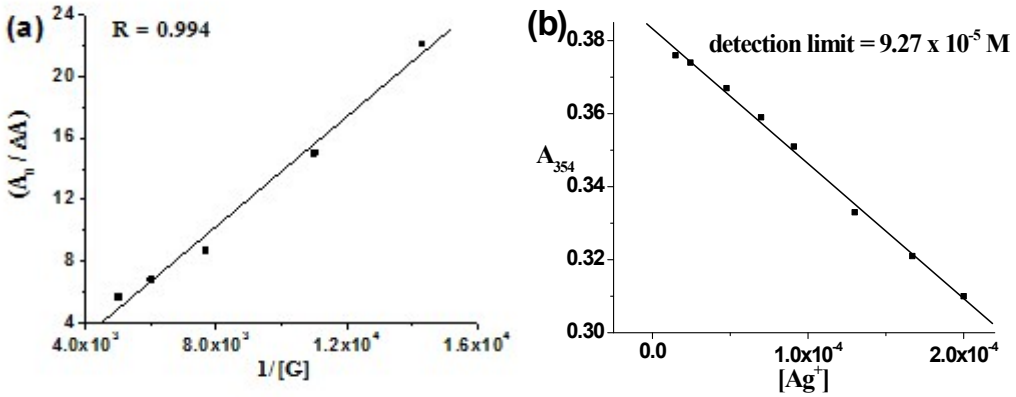

Fig. S18. (a) Benesi–Hilderband plot and (b) detection limit for **3** (c = 2.5 x 10^{-5} M) with Ag^{+} ion (c = 1.0 x 10^{-3} M) at 354 nm in 1,4-Dioxane/H_2O (2:1, v/v) from UV-vis titration.

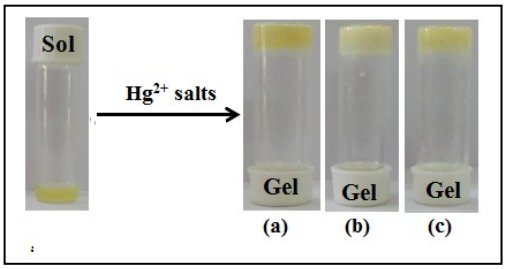

Fig. S19. Preparation of DMF-H_2O gel of **4** in presence of different Hg-salts; (a) $Hg(NO_3)_2$, (b) $Hg(ClO_4)_2$ and (c) $HgCl_2$.

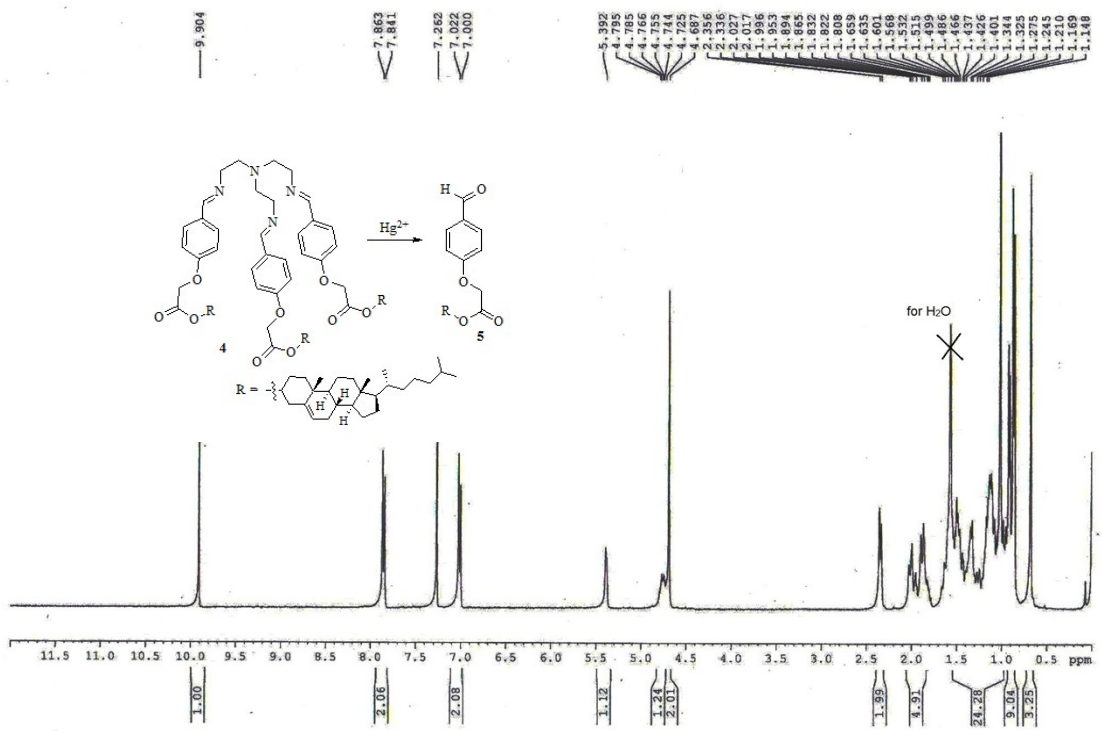

Fig. S20. ^1H NMR spectra ($CDCl_3$, 400 MHz) of the isolated product (compound **5**) obtained from the reaction of **4** with Hg^{2+} ion.

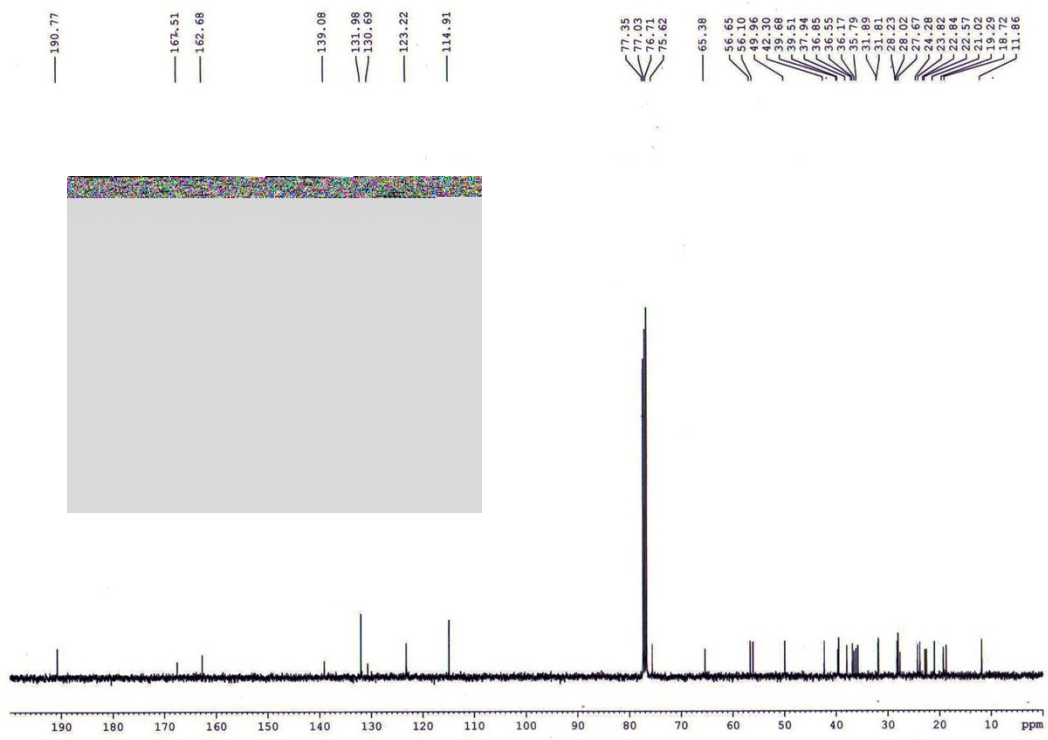

Fig. S21. ^{13}C NMR spectra ($CDCl_3$, 100 MHz) of the isolated product (compound **5**) obtained from the reaction of **4** with Hg^{2+} ion.

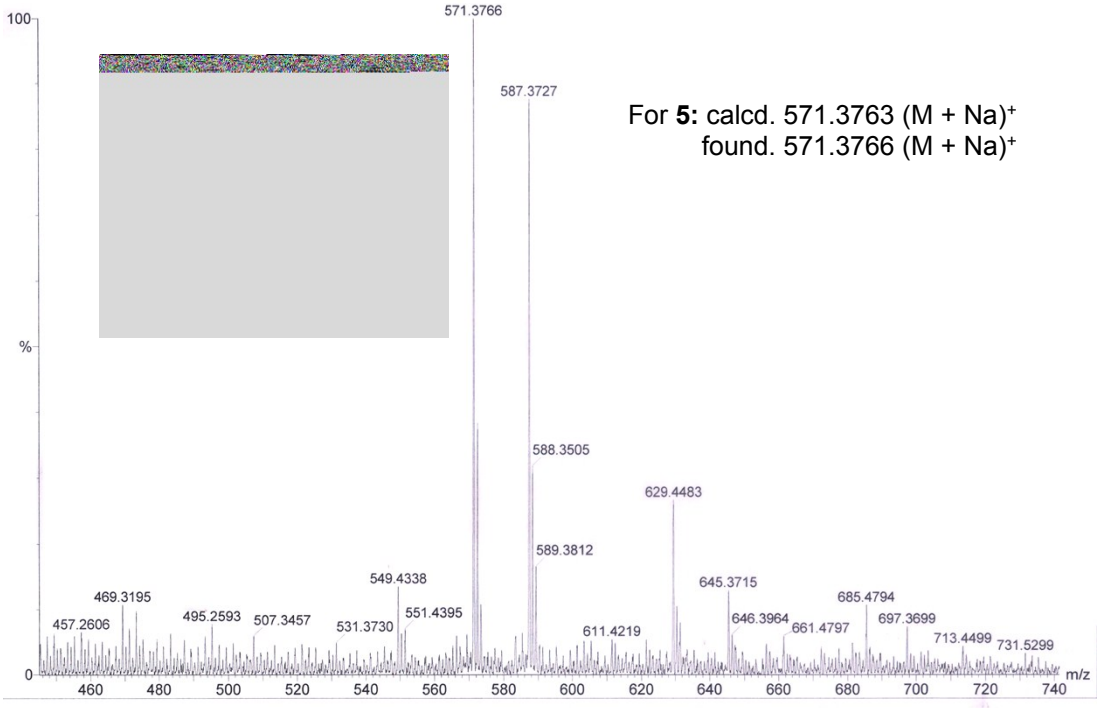

Fig. S22. HRMS spectra of the isolated product (compound **5**) obtained from the reaction of **4** with Hg^{2+} ion.

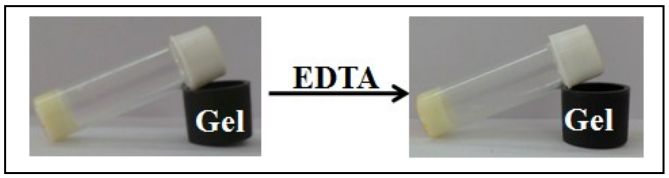

Fig. S23. Responsiveness of the Hg-gel of **4** in presence of EDTA.

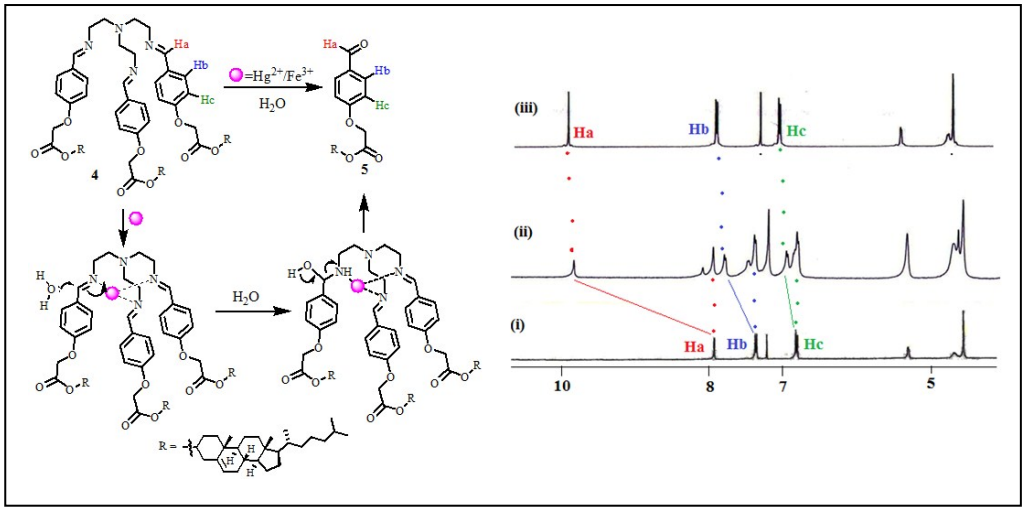

Fig. S24. Partial ^{1}H NMR spectra of (i) **4**, (ii) **4** with Fe^{3+} ion (1:1, after ~15 min) and (iii) **5** itself in $CDCl_3$.

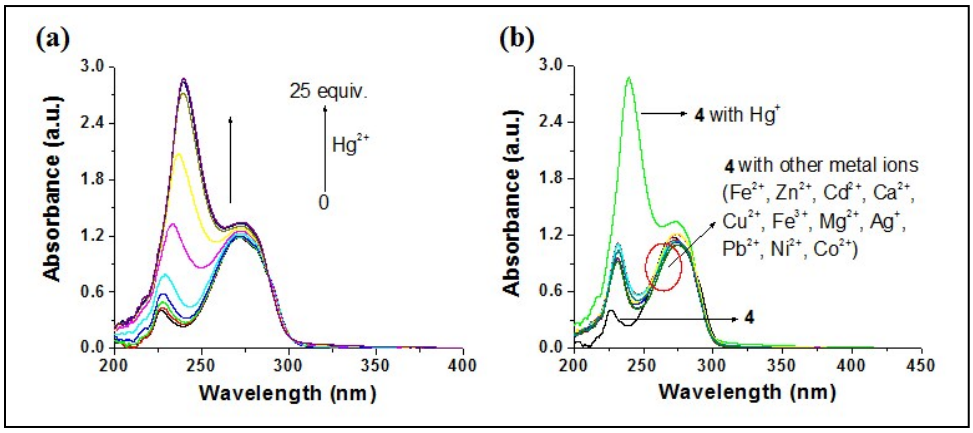

Fig. S25. Change in absorbance of **4** (c = 2.50 x 10^{-5} M) upon addition of 25 equiv. amounts of (a) Hg^{2+} and (b) different metal ions (as perchlorate salts, c = 1.0 x 10^{-3} M) in DMF/H_2O (1:1, v/v).

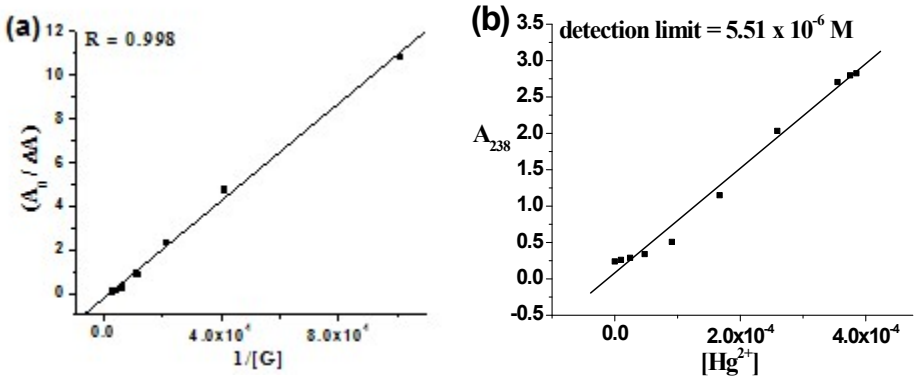

Fig. S26. (a) Benesi–Hilderband plot and (b) detection limit for **4** (c = 2.5 x 10^{-5} M) with Hg^{2+} ion (c = 1.0 x 10^{-3} M) at 238 nm in DMF/H_2O (1:1, v/v) from UV-vis titration.

Table S4. Binding constants and detection limit values for the metal ligand complexes.

Metal ligand complex	Binding constant values (M^{-1})	
	From UV-vis titration	
2 – Ag^+	K = 1.55 x 10^3	
3 – Ag^+	K = 2.23 x 10^3	

Metal ligand complex	Detection limit values (M)	
	From UV-vis titration	
2 – Ag^+	3.27 x 10^{-5}	
3 – Ag^+	9.27 x 10^{-5}	
4 – Hg^{2+}	5.51 x 10^{-6}	

Table S5: Chemodosimeters based on Hg^{2+} ion-induced imine bond hydrolysis mechanism

Structure	Solvent	Sensing mechanism	Interfering metal ions	Detection limit for Hg^{2+} (M)	Ref.
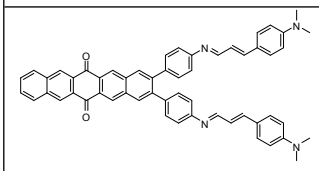	THF–H_2O (9.5 : 0.5, v : v) buffered with HEPES, pH = 7	Fluorescence enhancement	-	2.8 x 10^{-10}	*Dalton Trans.*, 2013, **42**, 15063.
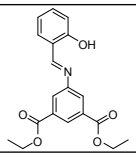	MeOH/ H_2O (9:1, v/v)	Fluorescence enhancement	-	8 x 10^{-10}	*Inorg. Chem.*, 2014, **53**, 4944.
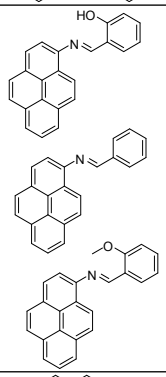	CH_3CN:H_2O (9:1)	Fluorescence enhancement	- Pb^{2+}, Fe^{2+} Pb^{2+}, Fe^{2+}, Fe^{3+}	- - -	*Arkivoc,* 2010, **7**, 170.
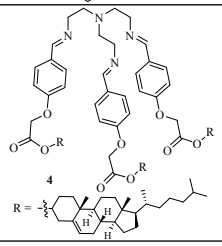	DMF : H_2O = (1 : 1, v/v)	Sol to gel transition Chemodosimetric approach	-	5.51 x 10^{-6}	*Present work*

^{1}H NMR of 1 ($CDCl_3$, 400 MHz)

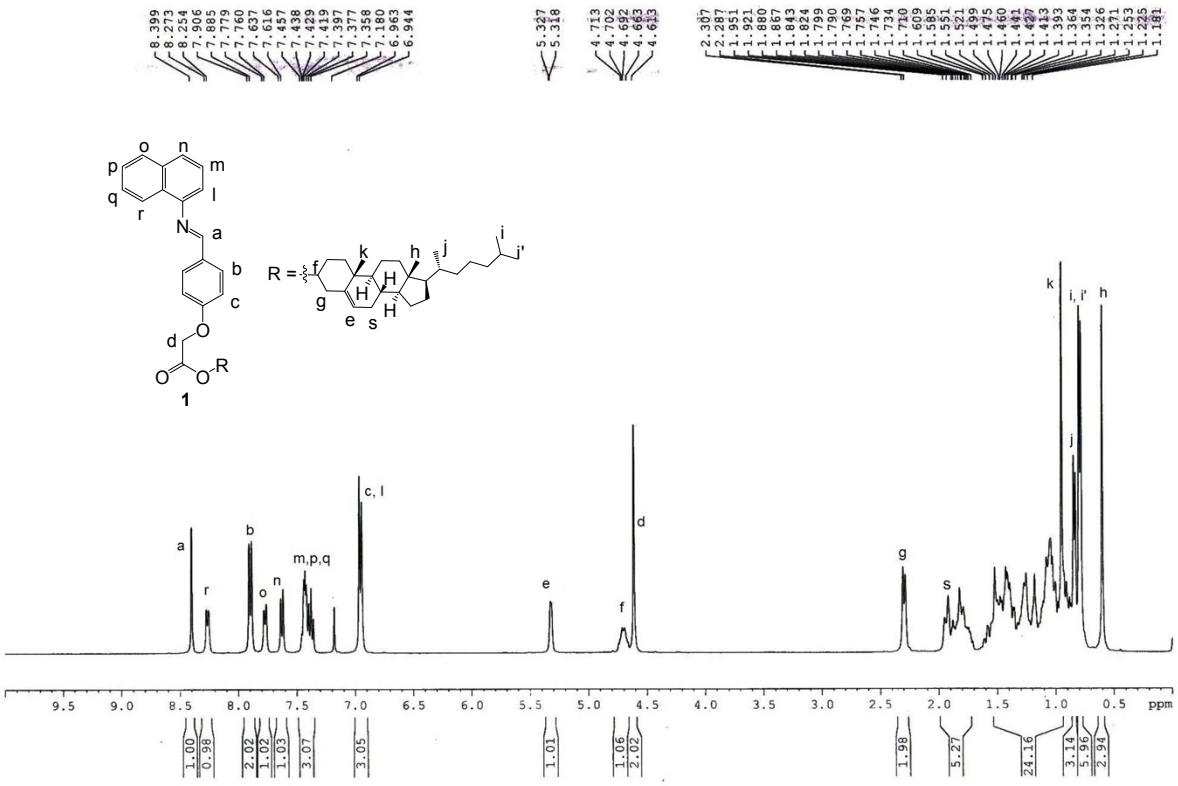

^{13}C NMR of 1 ($CDCl_3$, 100 MHz)

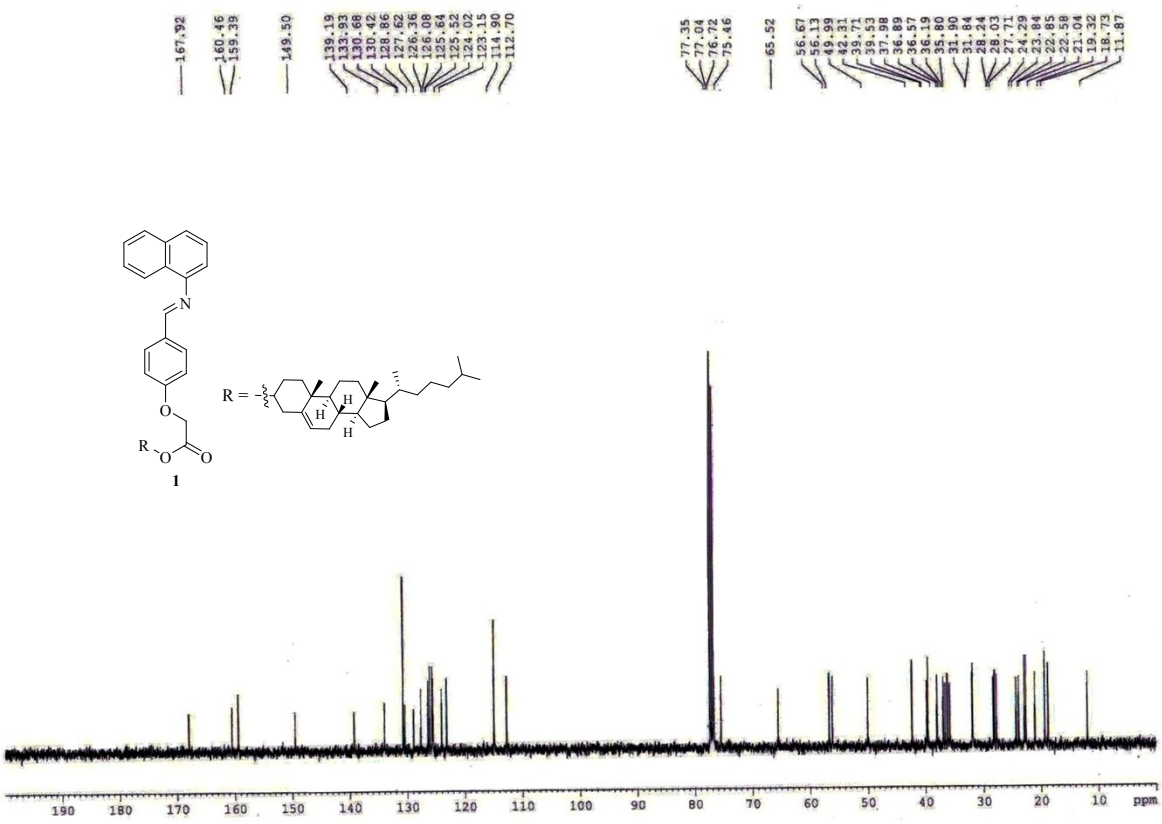

Mass spectrum of 1.

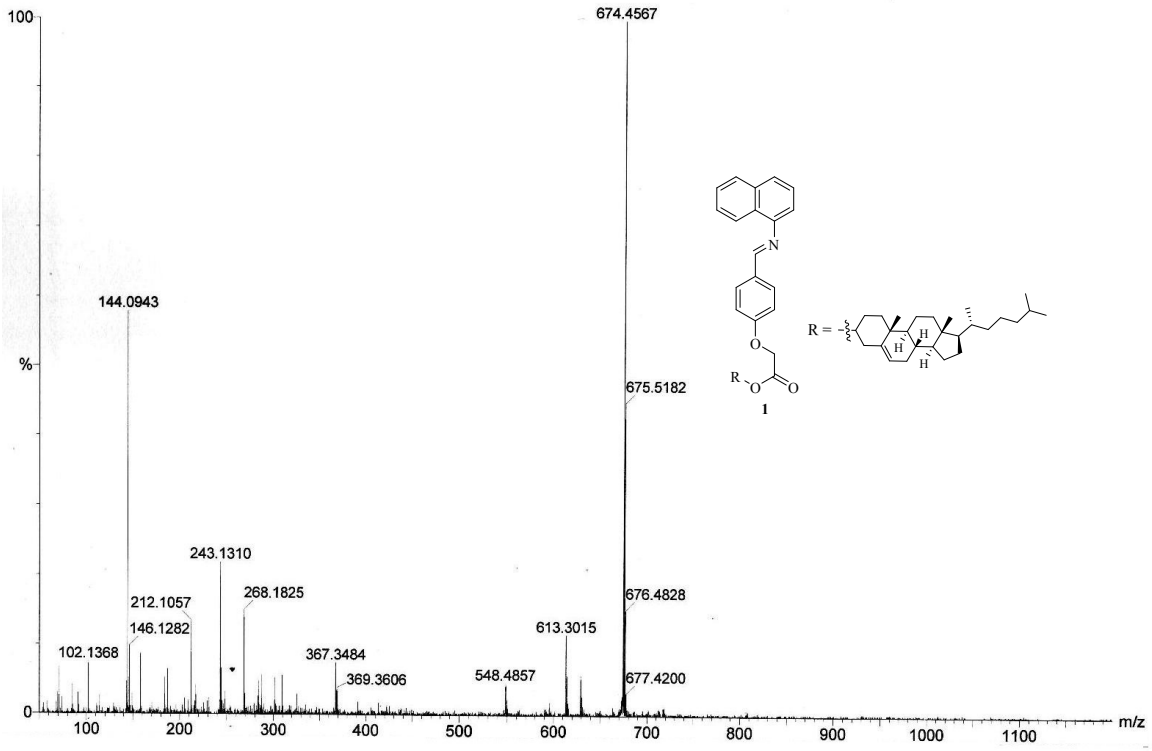

COSY spectrum of 1 ($CDCl_3$, 500 MHz)

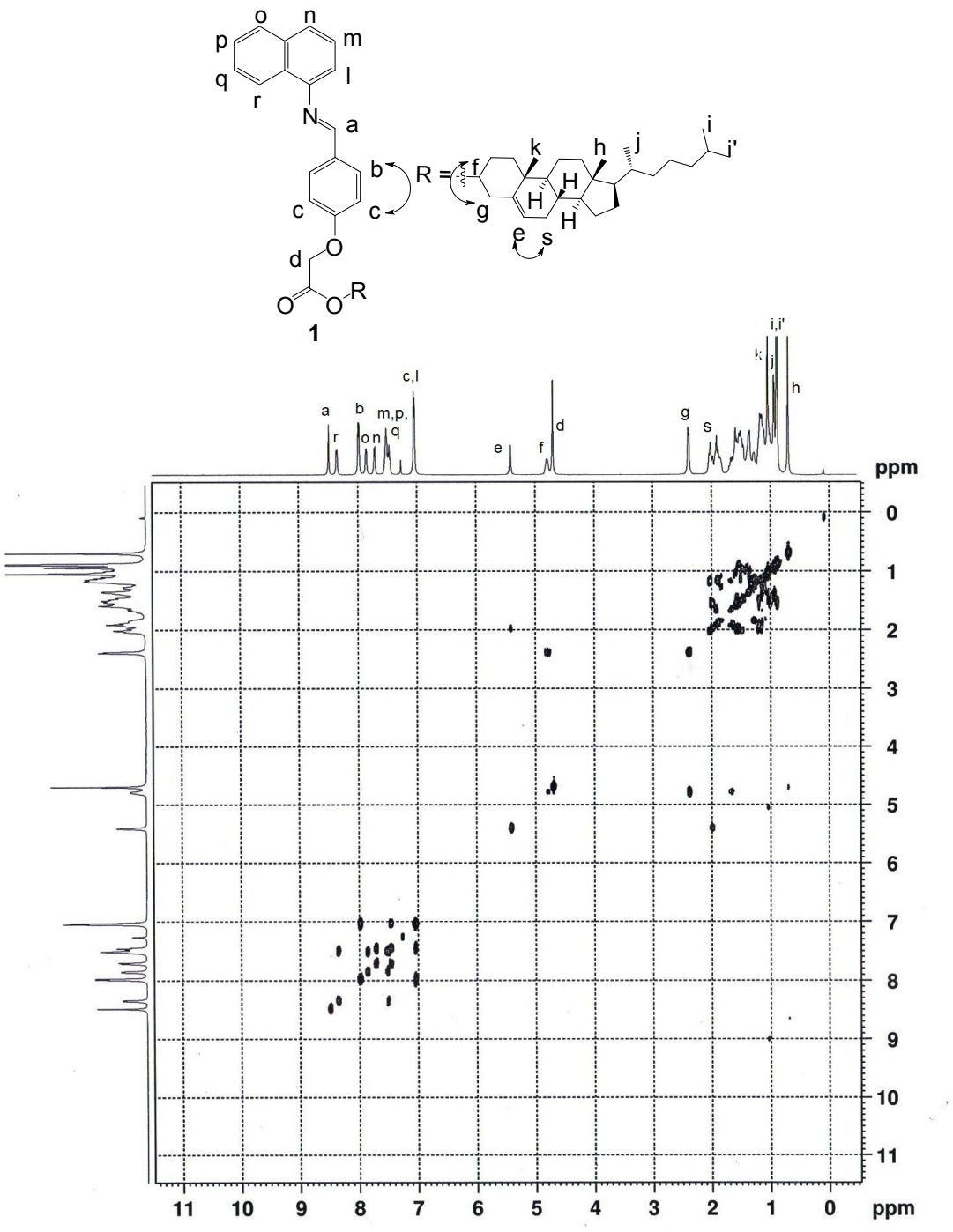

NOESY spectrum of 1 ($CDCl_3$, 400 MHz)

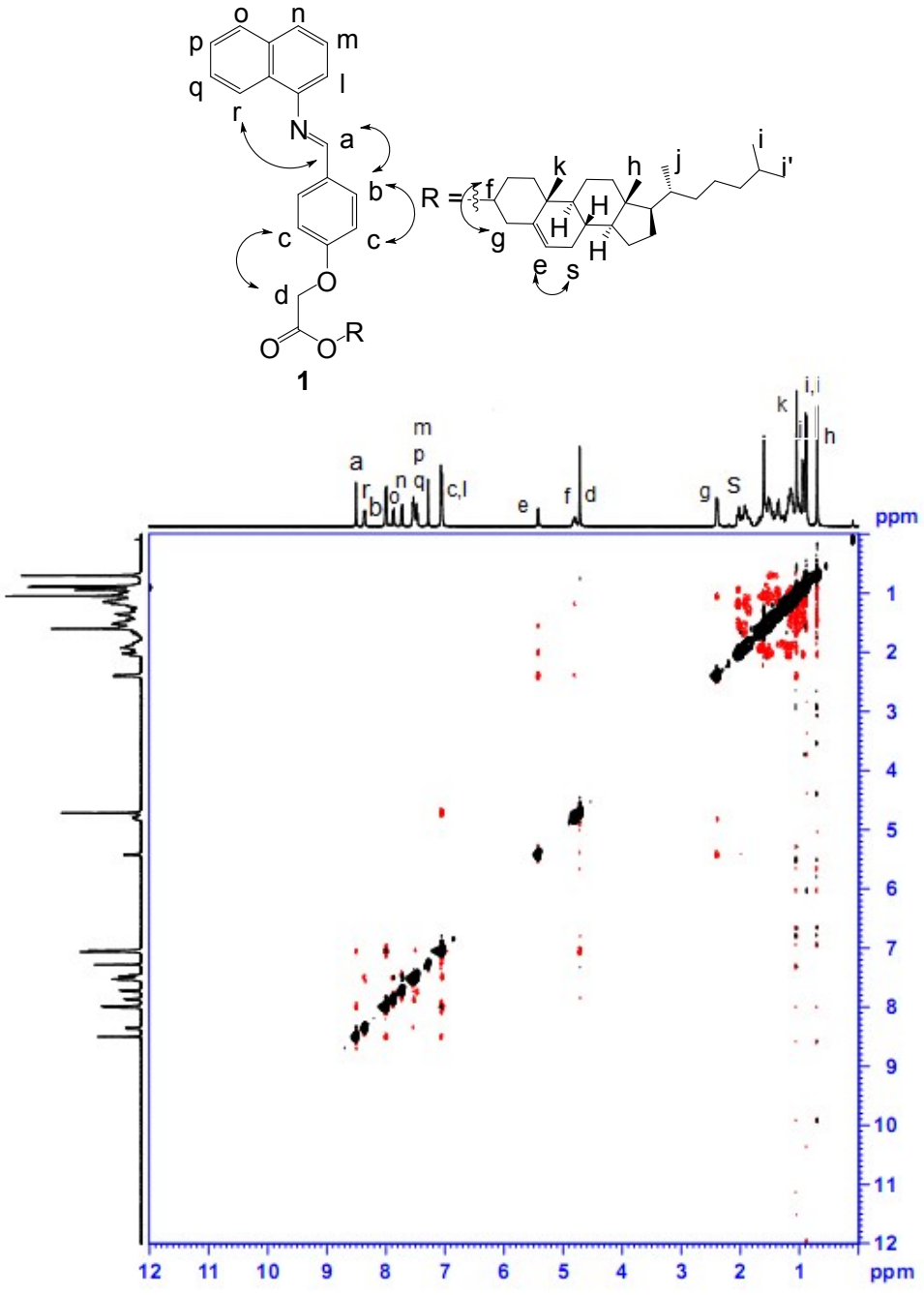

Partial NOESY spectrum of 1 ($CDCl_3$, 400 MHz)

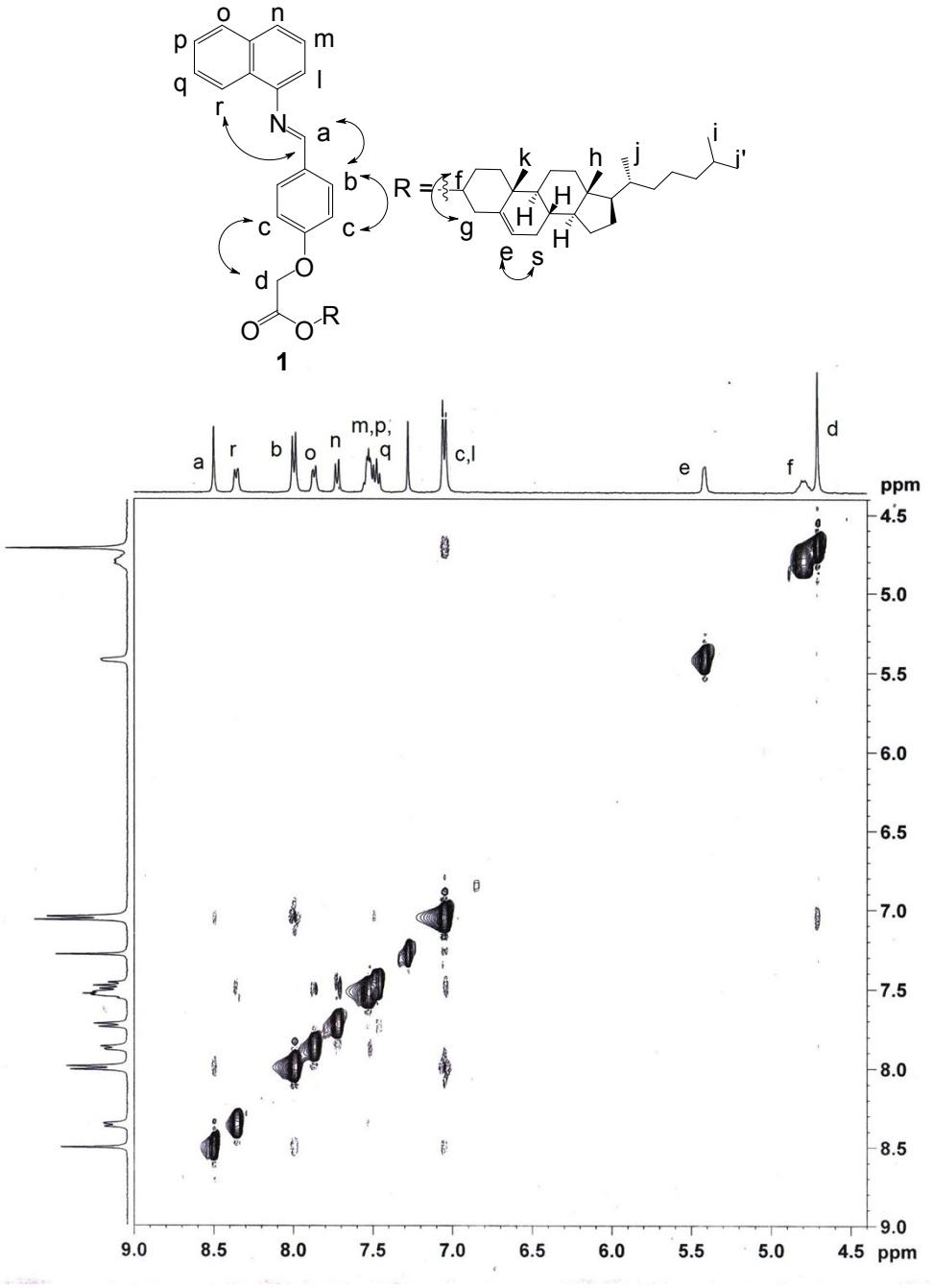

^{1}H NMR of 2 ($CDCl_3$, 400 MHz)

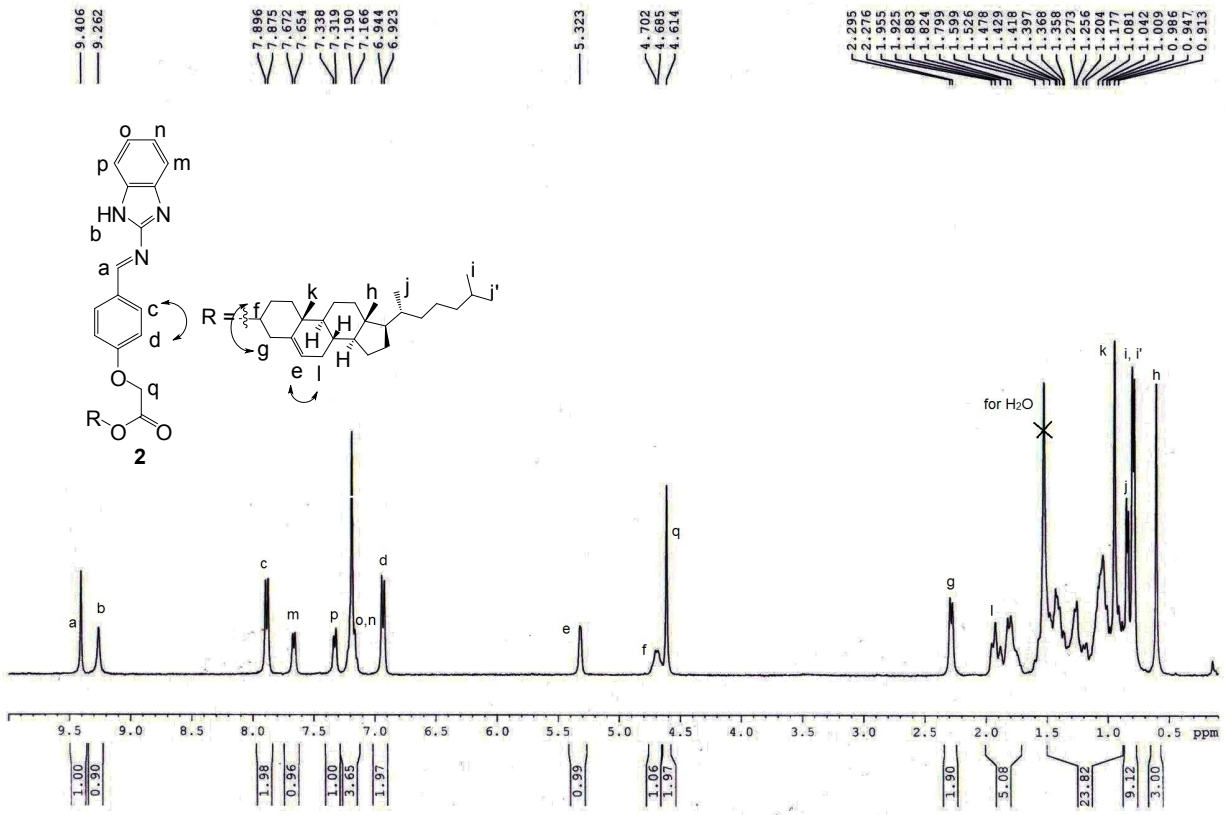

^{13}C NMR of 2 ($CDCl_3$, 100 MHz)

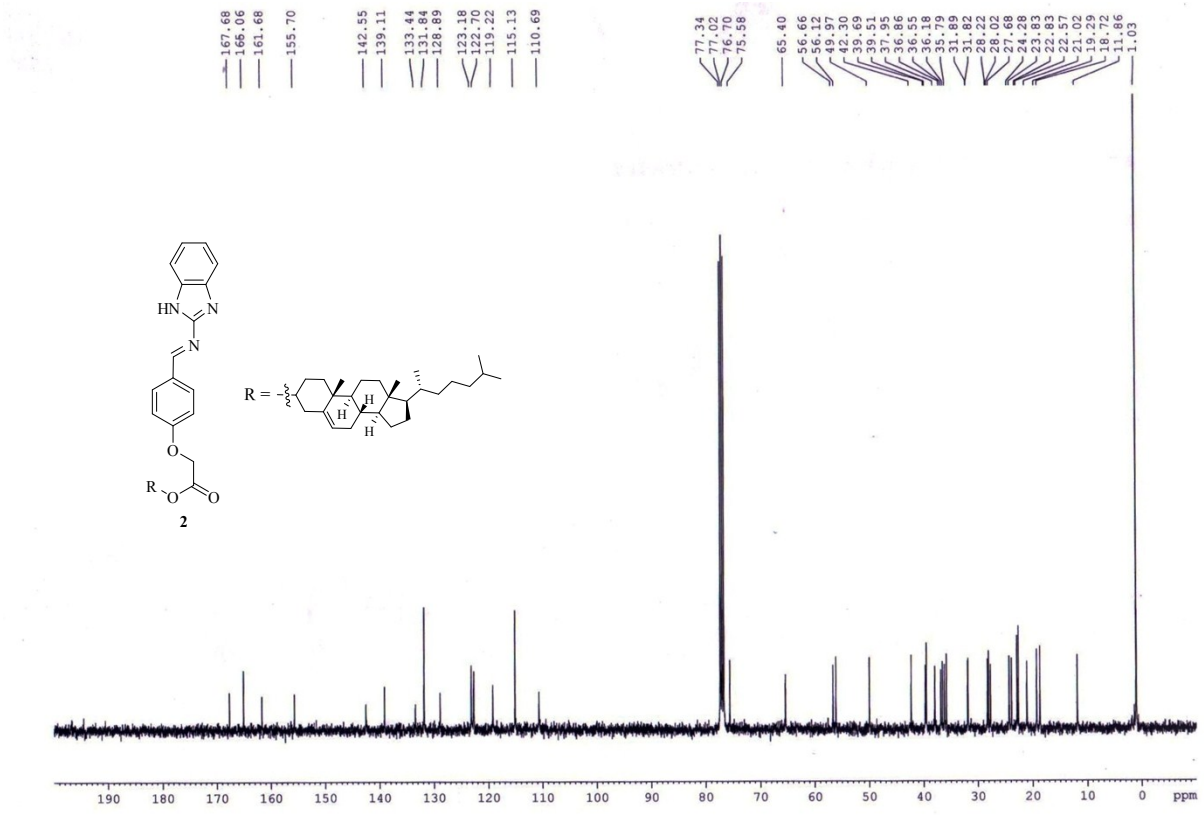

Mass spectrum of 2.

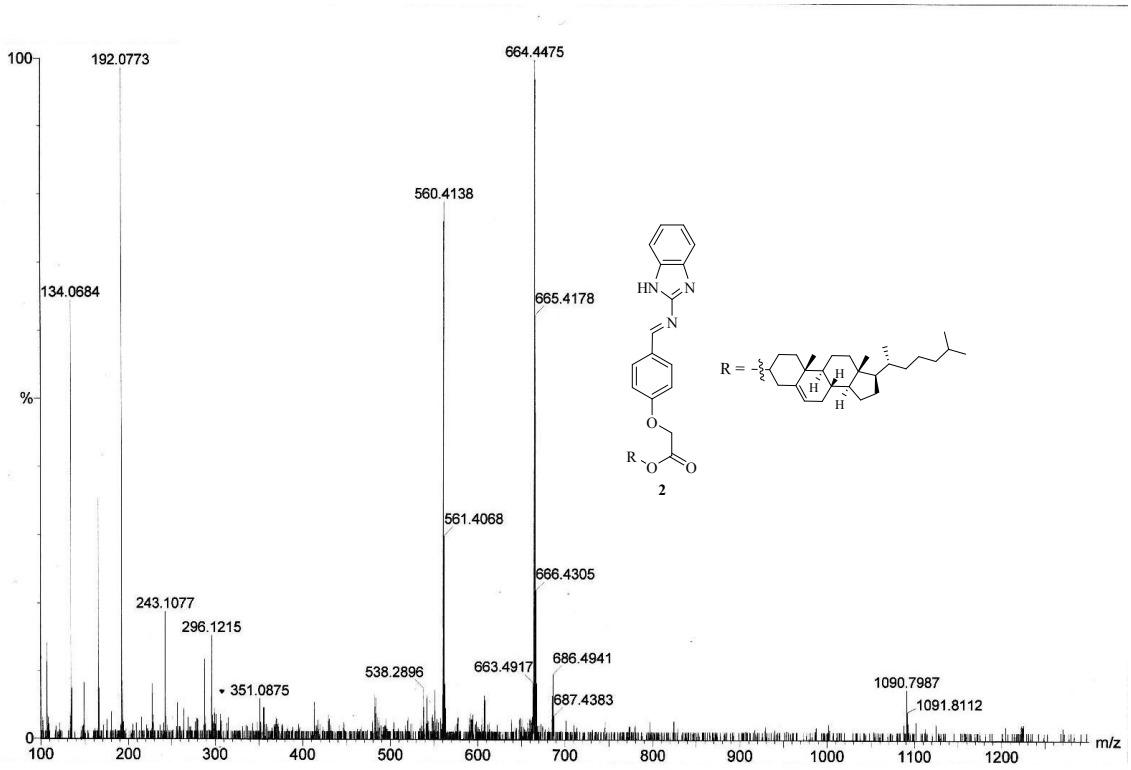

COSY spectrum of 2 ($CDCl_3$, 500 MHz)

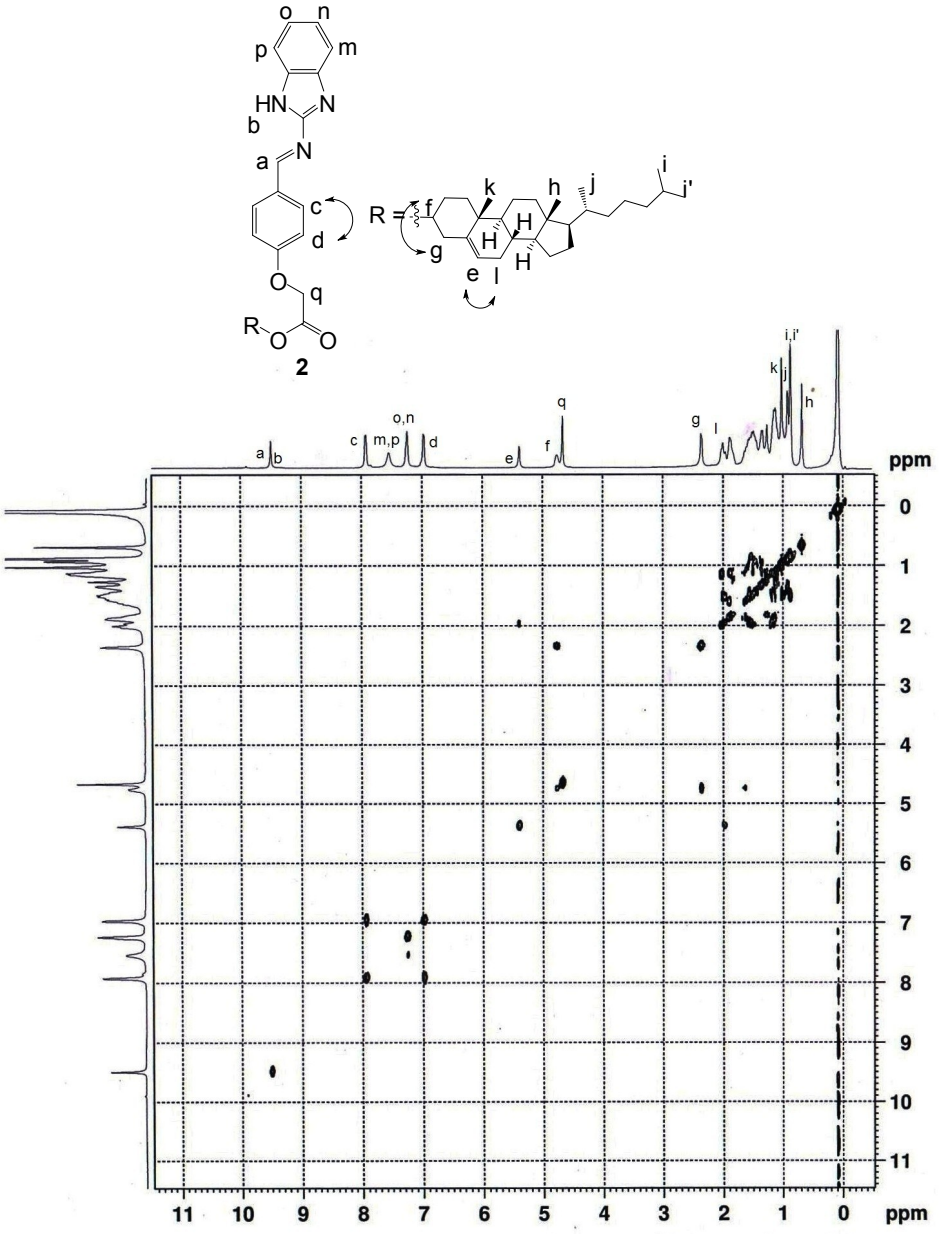

^{1}H NMR of 3 ($CDCl_3$, 400 MHz)

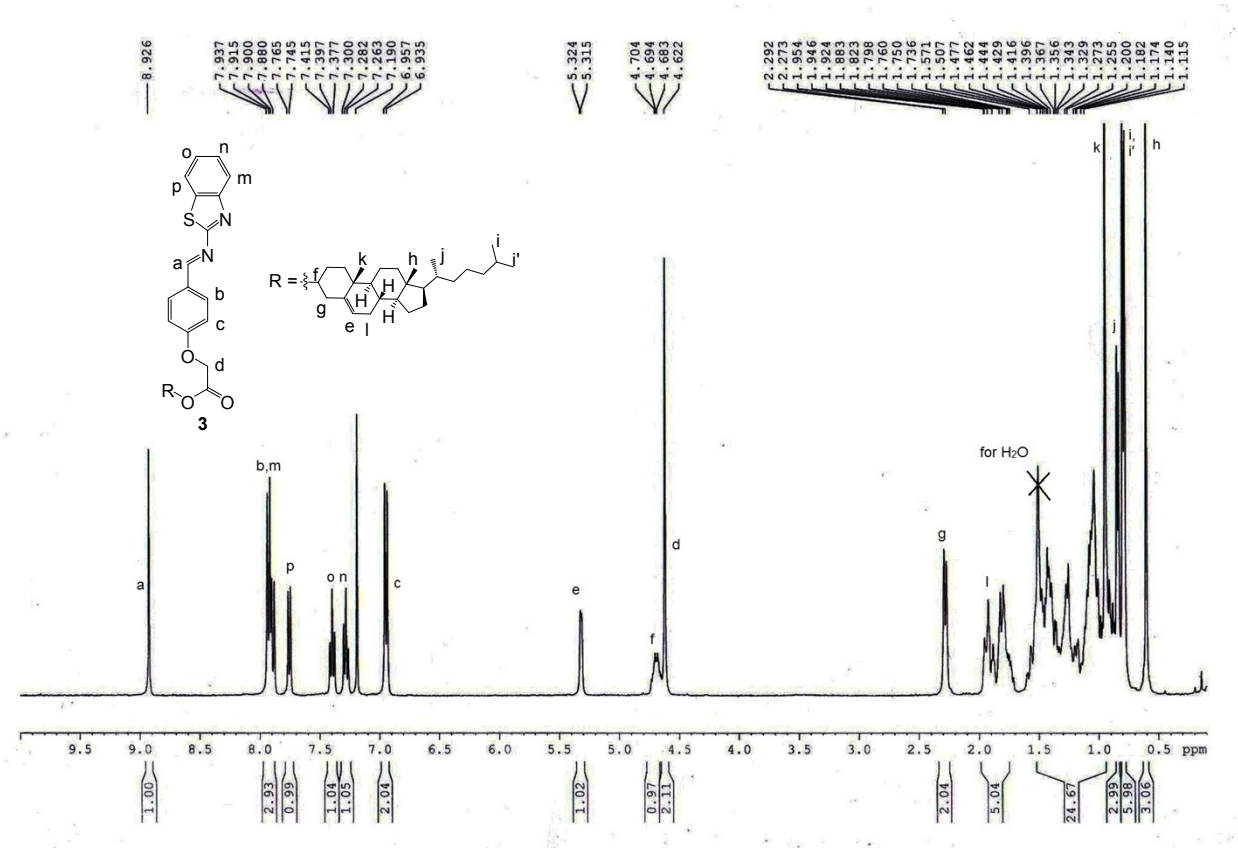

^{13}C NMR of 3 ($CDCl_3$, 100 MHz)

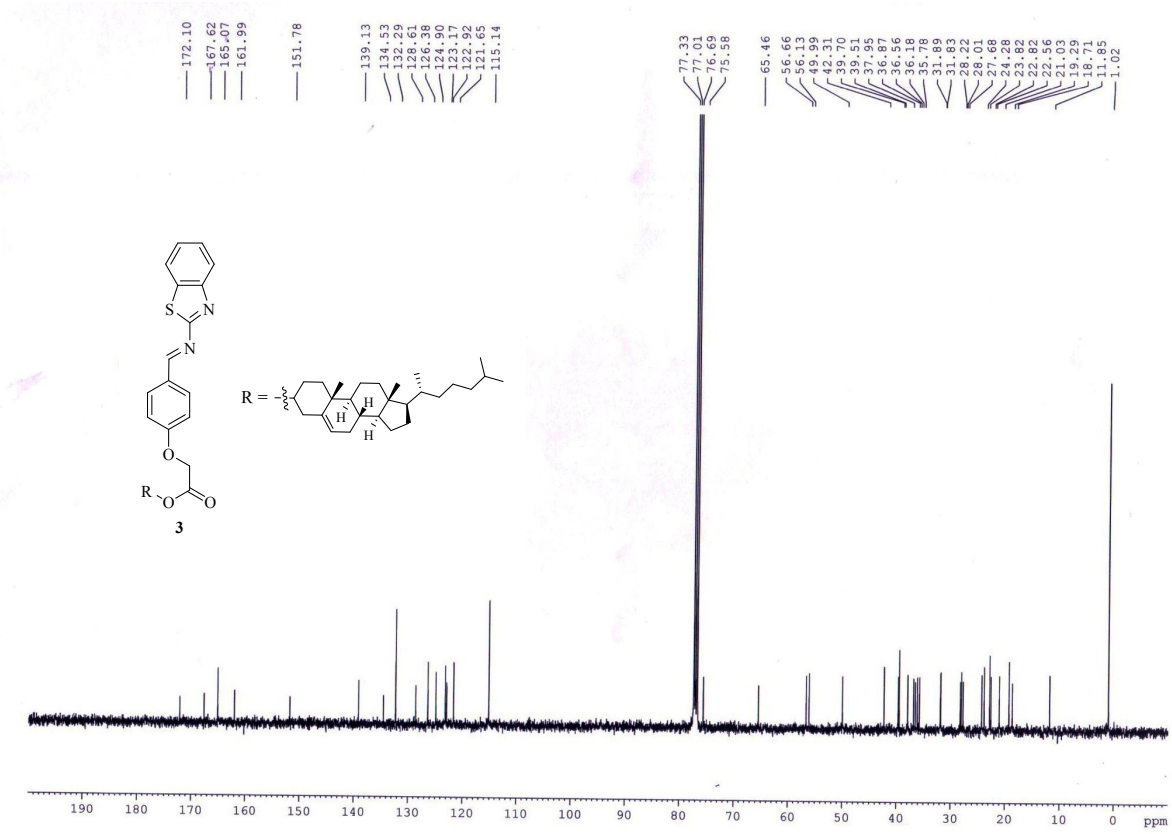

Mass spectrum of 3.

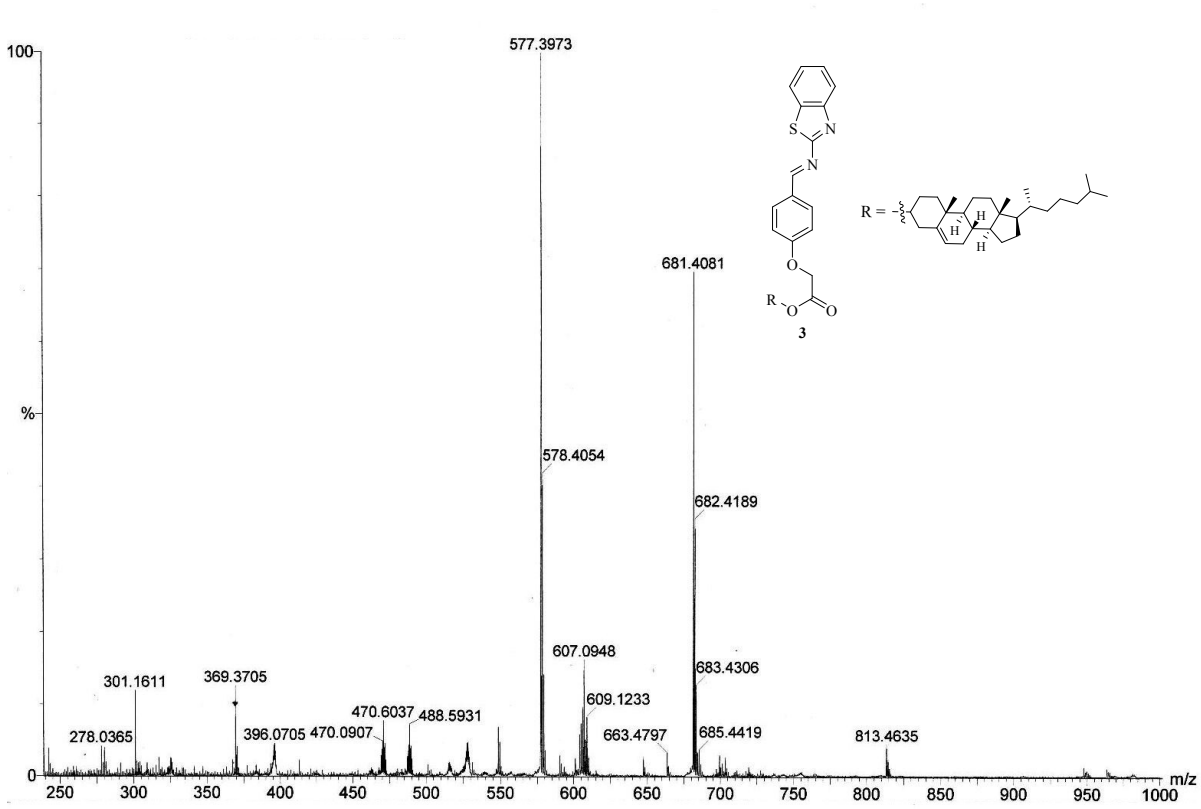

COSY spectrum of 3 ($CDCl_3$, 500 MHz)

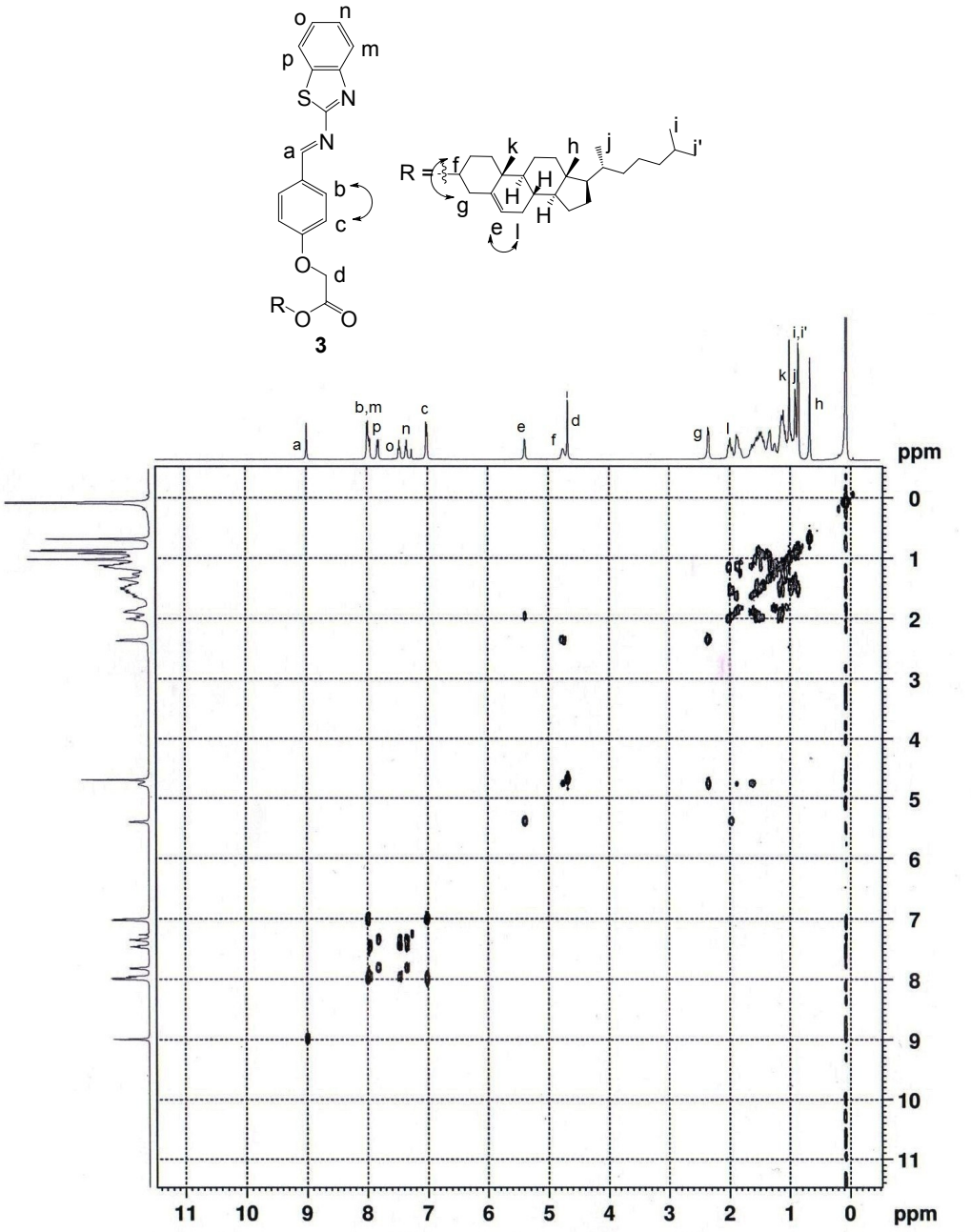

^{1}H NMR of 4 ($CDCl_3$, 400 MHz)

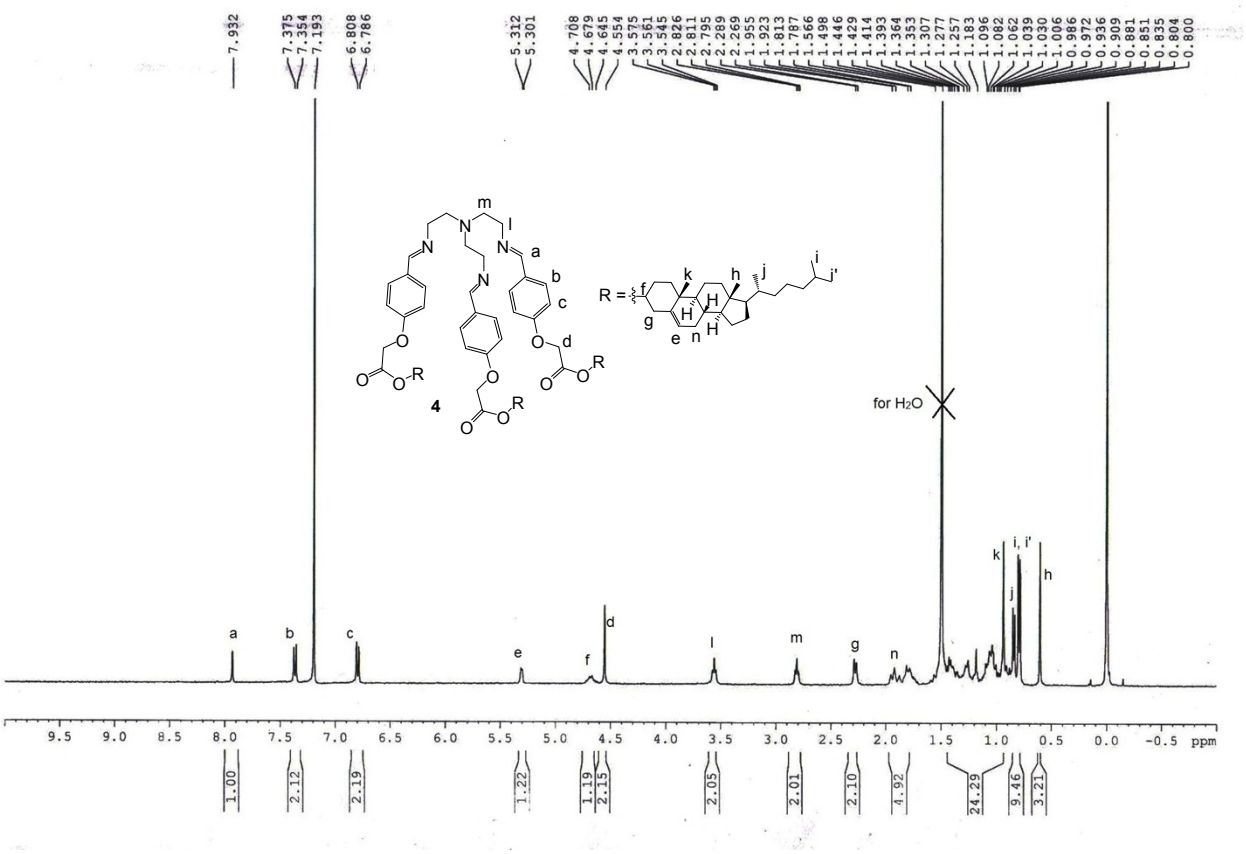

^{13}C NMR of 4 ($CDCl_3$, 100 MHz)

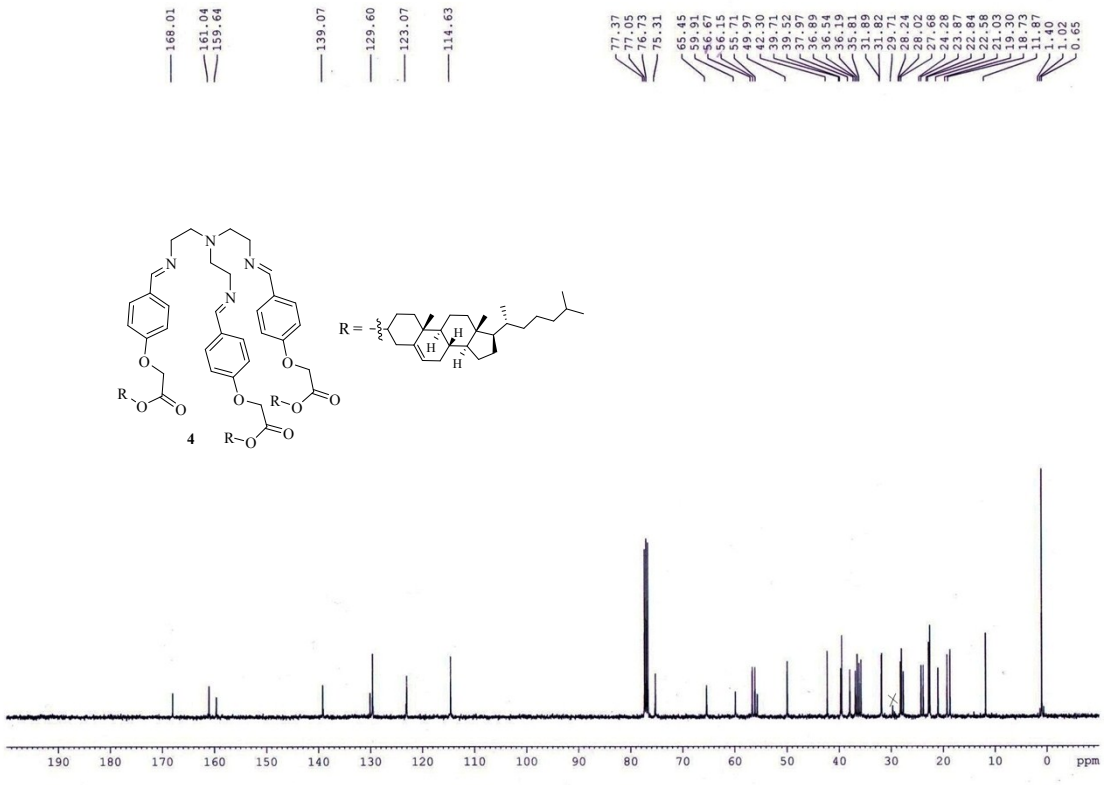

Mass spectrum of 4.

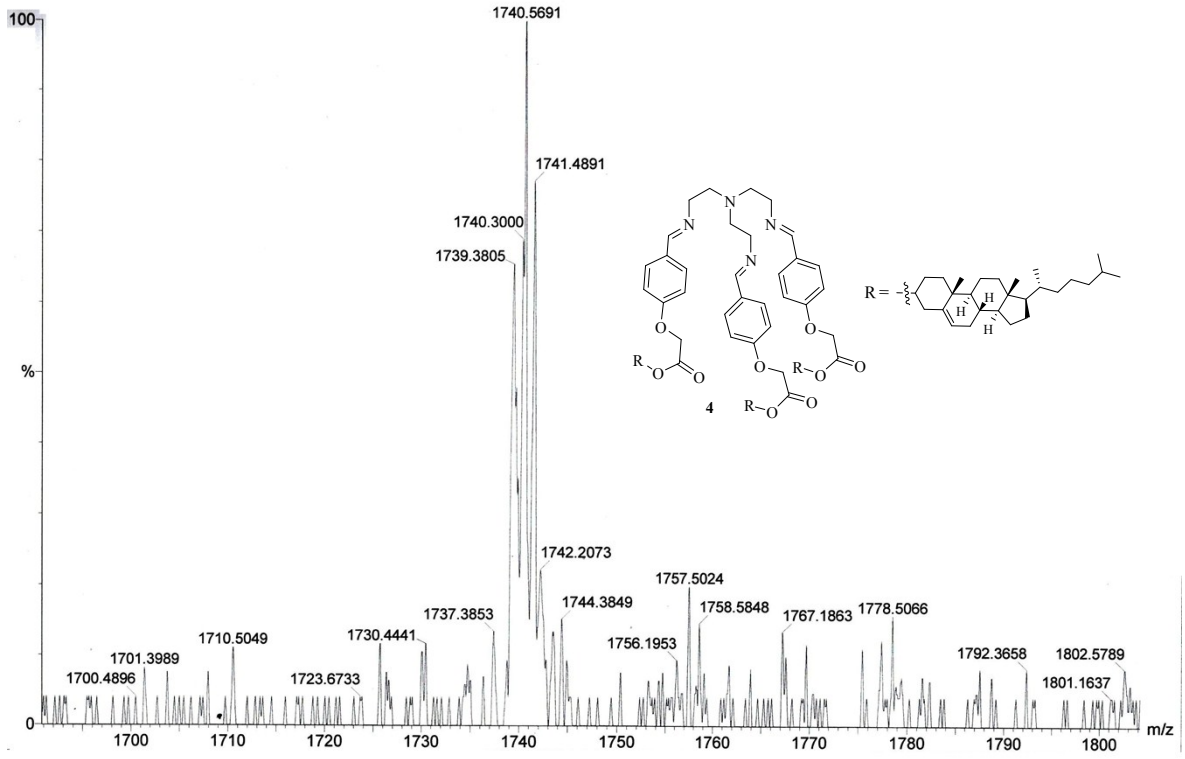

COSY spectrum of 4 ($CDCl_3$, 500 MHz)

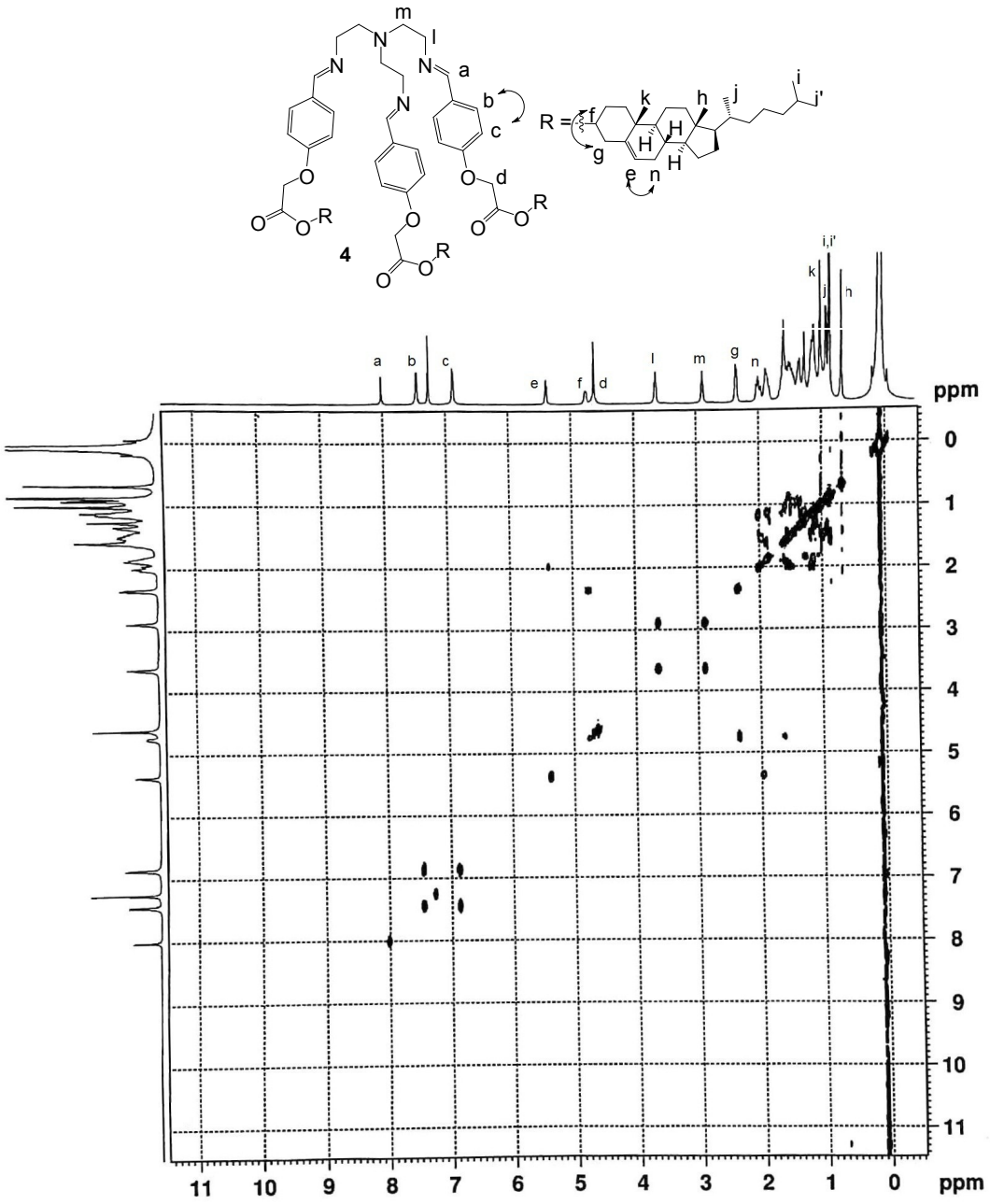

NOESY spectrum of 4 ($CDCl_3$, 400 MHz)

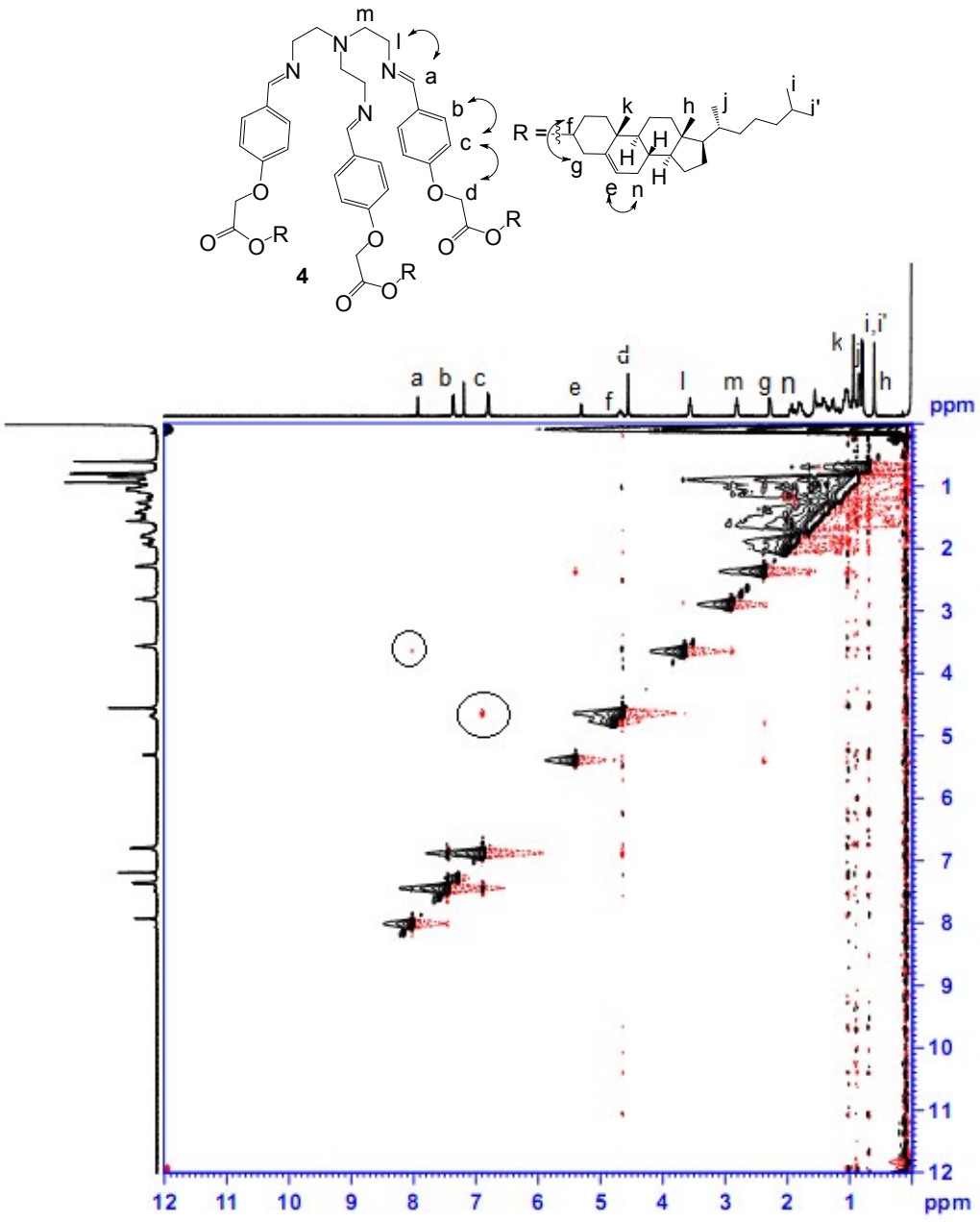

Partial NOESY spectrum of 4 ($CDCl_3$, 400 MHz)

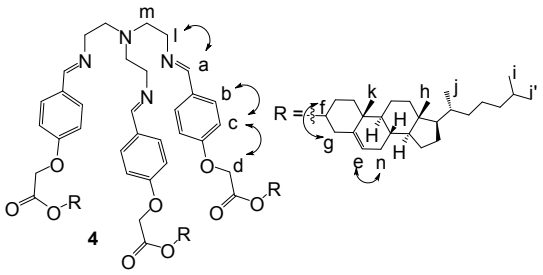

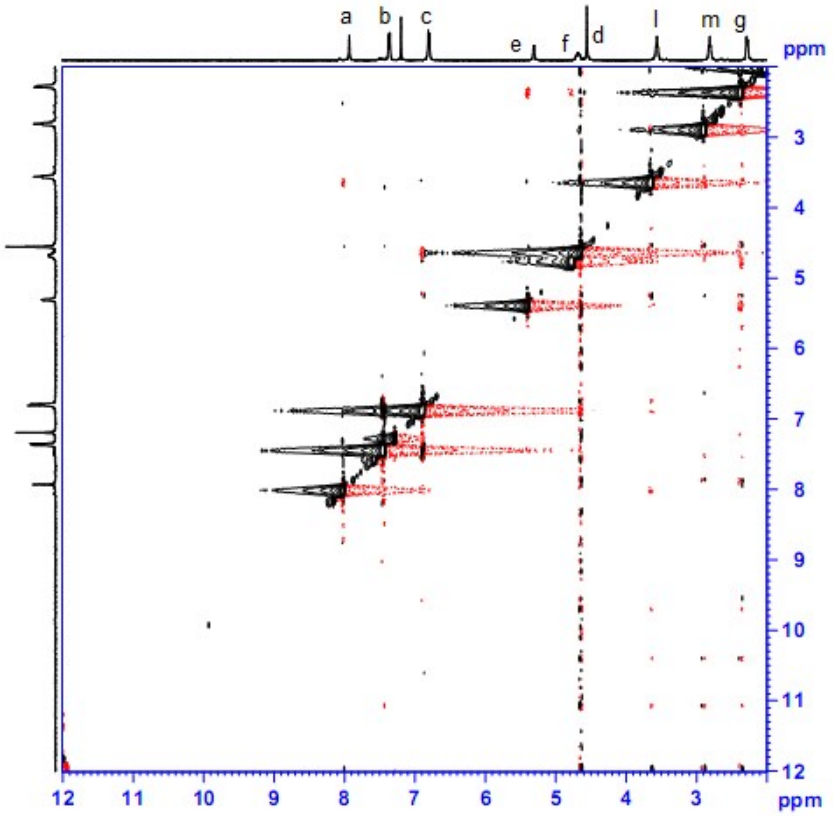

^{1}H NMR of 5 ($CDCl_3$, 400 MHz)

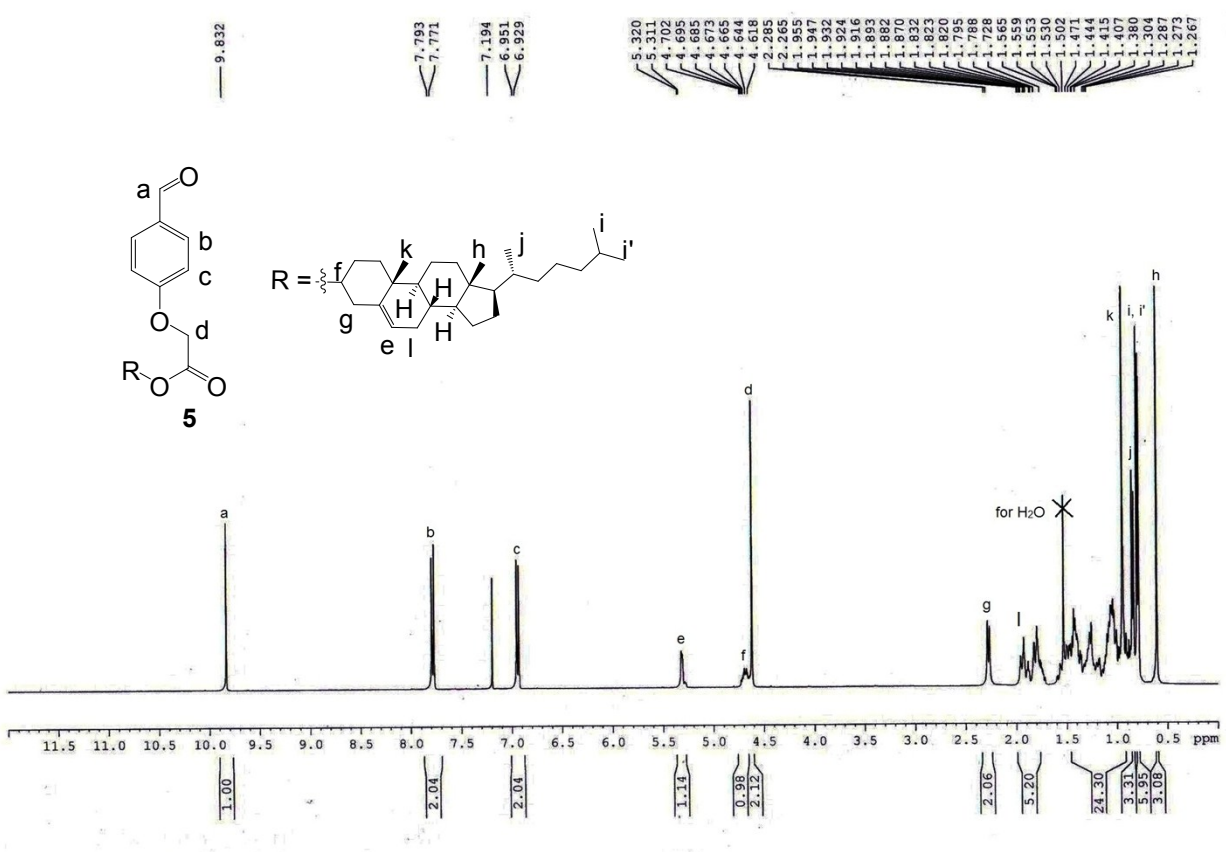

^{13}C NMR of 5 ($CDCl_3$, 100 MHz)

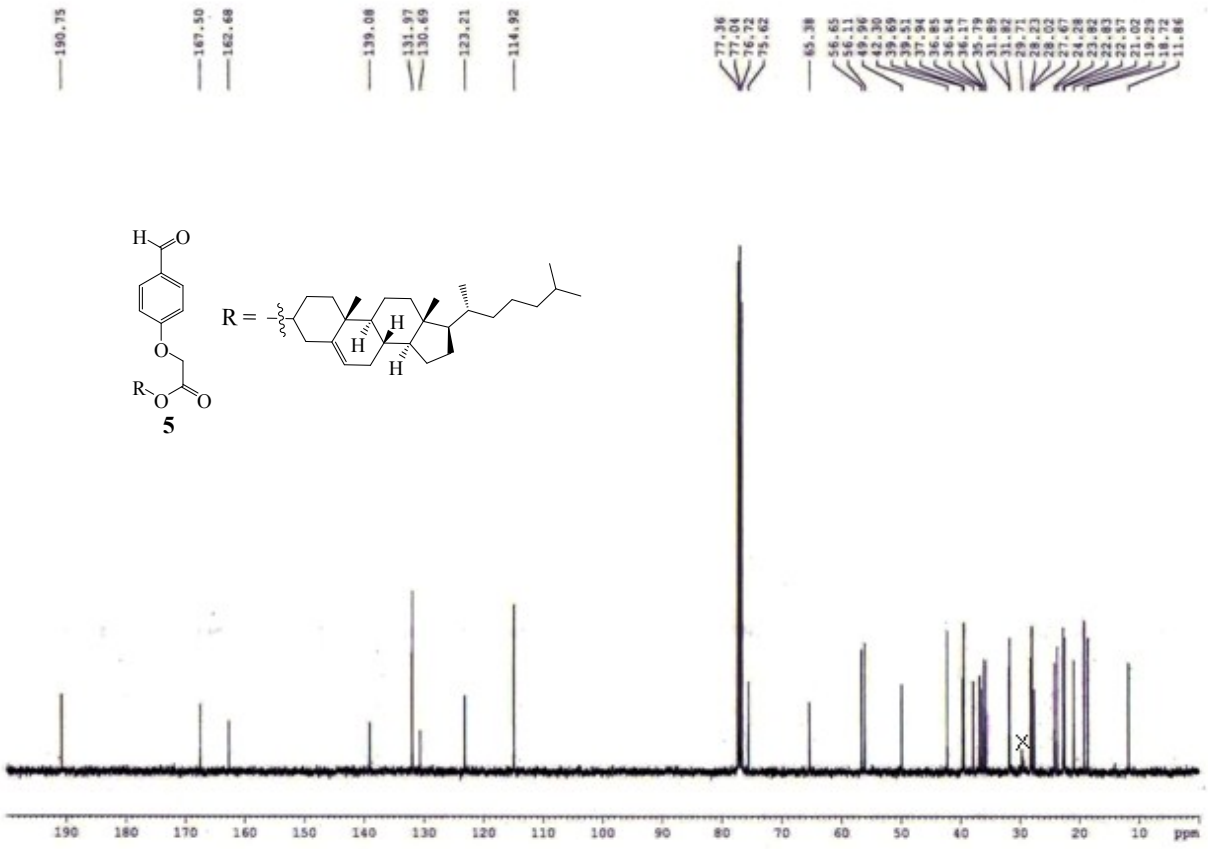

Mass spectrum of 5.

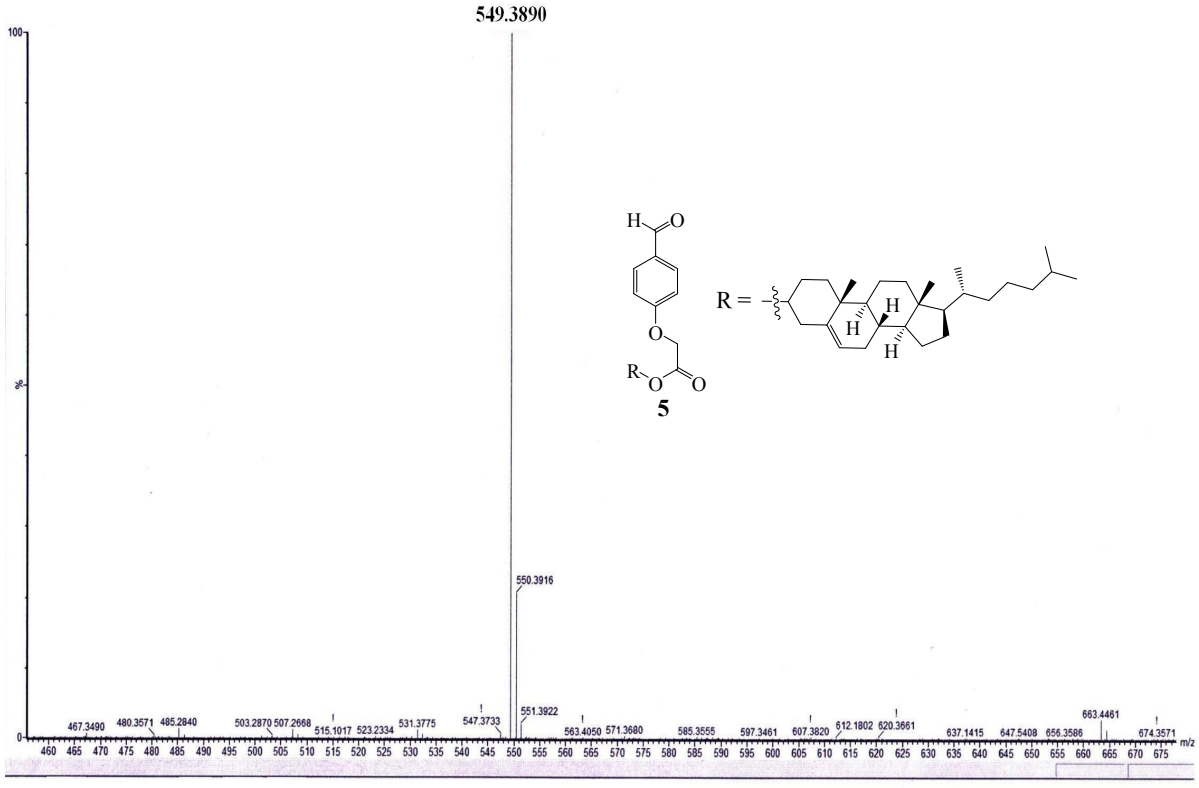

5

COSY spectrum of 5 ($CDCl_3$, 500 MHz)

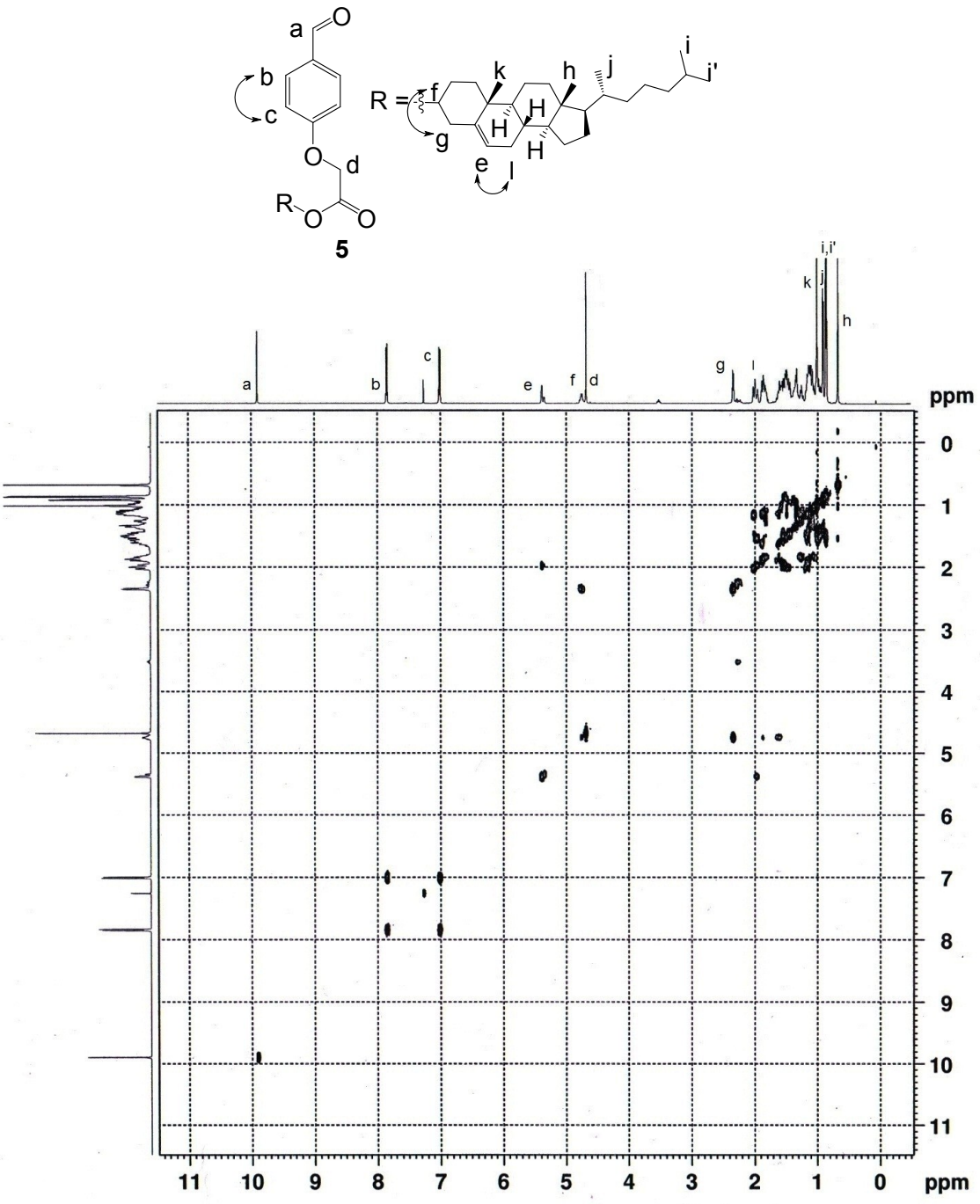

NOESY spectrum of 5 ($CDCl_3$, 400 MHz)

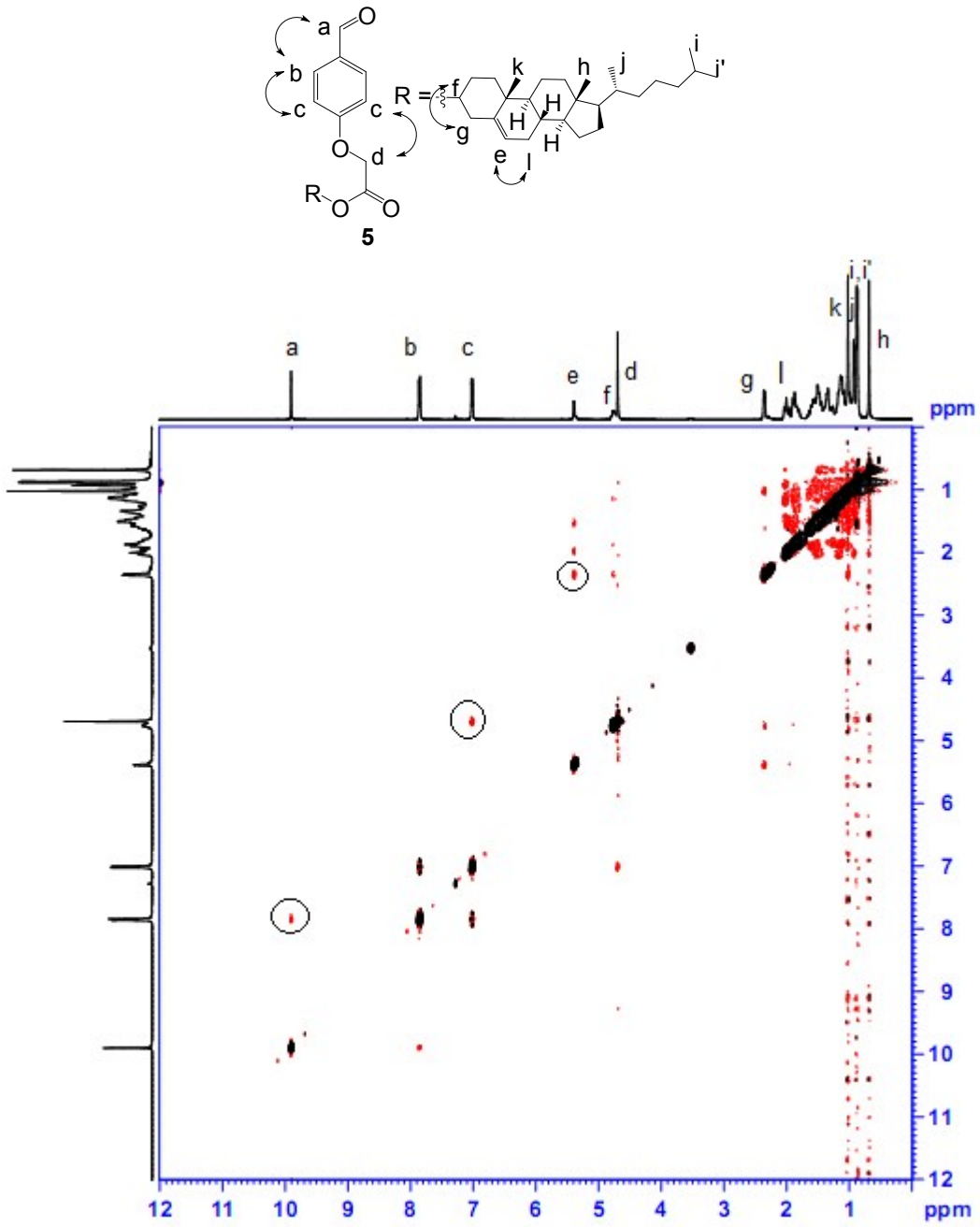

Partial NOESY spectrum of 5 ($CDCl_3$, 400 MHz)

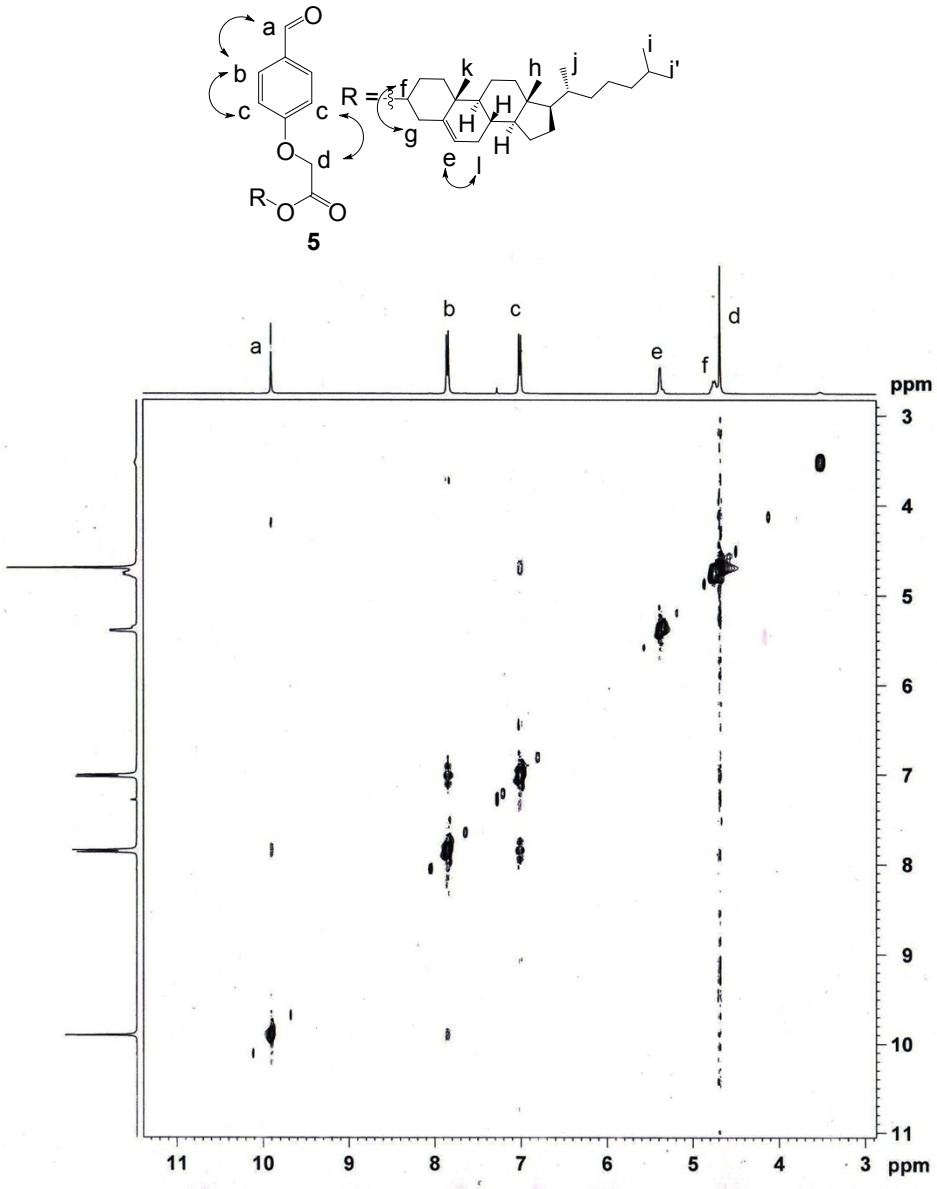

Partial FTIR spectra of compounds (a) 1, (b) 2, (c) 3, (d) 4 and (e) 5.